INVESTIGATION ON MEDIA PACK CONFIGURATIONS FOR AIR FILTRATION DEVICES
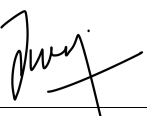
KHAW JI WEI

A project report submitted in partial fulfilment of the requirements for the award of Bachelor of Engineering (Honours) Mechanical Engineering

Lee Kong Chian Faculty of Engineering and Science
Universiti Tunku Abdul Rahman

September 2020

DECLARATION

I hereby declare that this project report is based on my original work except for citations and quotations which have been duly acknowledged. I also declare that it has not been previously and concurrently submitted for any other degree or award at UTAR or other institutions.

Signature   :

Name   : Khaw Ji Wei

ID No.   : 16UEB06865

Date   : 14/9/20

APPROVAL FOR SUBMISSION

I certify that this project report entitled **"INVESTIGATION ON MEDIA PACK CONFIGURATIONS FOR AIR FILTRATION DEVICES"** was prepared by **KHAW JI WEI** has met the required standard for submission in partial fulfilment of the requirements for the award of Bachelor of Engineering (Honours) Mechanical Engineering at Universiti Tunku Abdul Rahman.

Approved by,

Signature   :   _____

Supervisor   :   Dr. Poon Hiew Mun
                  _____

Date   :   14/9/20
                  _____

The copyright of this report belongs to the author under the terms of the copyright Act 1987 as qualified by Intellectual Property Policy of Universiti Tunku Abdul Rahman. Due acknowledgement shall always be made of the use of any material contained in, or derived from, this report.

ACKNOWLEDGEMENTS

I would like to thank everyone who had contributed to the successful completion of this project. I would like to express my gratitude to my research supervisor, Dr. Poon Hiew Mun for her invaluable advice, guidance and her enormous patience throughout the development of the research.

In addition, I would also like to express my gratitude to my loving parents and friends who had helped and given me encouragement throughout the entire project.

Last but not least, I would also like to express my sincere gratitude to UTAR for giving me an opportunity to be involved in this research project.

ABSTRACT

The increasing need for clean air has highlighted the importance of air filtration devices in improving air quality. Generally, resistance is produced when air is moved through an air filter media which contains large density of fibres. In air filtration system, one of the performance parameters is indicated by the amount of pressure drop across the filter media. Thus, this study aims to investigate the influence of media pack configuration on the performance of air filtration device. In this study, the filter media was made into pleated model by using Solidworks, while the fluid flow was simulated on a commercially available filter media by using Ansys Fluent software. The filter media was treated as a porous medium throughout the entire study. To ensure that minimum pressure drop is attained, the effects of pleat shape, pleat distance, and pleat height on the filter media were examined. It was found that when the flat sheet filter media was made into pleated shape, the pressure drop was reduced due to increased filtration area. However, pressure drop would rise with viscous drag effect when pleat space became too narrow that the contraction and expansion of flow was significant. The typical U-shaped curve generated in the results is in strong agreement with the findings of Chen, Pui and Liu (1995). Therefore, this implies that the minimum pressure drop is attained when trade-off between the effects of filtration area and viscous drag on media is achieved by the optimal interaction between pleat distance and pleat height.

TABLE OF CONTENTS

LIST OF TABLES

LIST OF FIGURES

LIST OF SYMBOLS / ABBREVIATIONS

V	face velocity, m/s
Y	pleat distance, m
L	pleat height, m
s	thickness, m
x	distance from tip of pleat, m
N	number of pleats per filter
D	hydraulic diameter, m
A	area, m^2
P	perimeter of duct, m
S_i	source term
C_2	inertial resistance, m^{-1}
θ	pleat angle, °
ρ	density, kg/m^3
μ	dynamic viscosity, kg/(m·s)
α	permeability, m^2
Δp	pressure drop, Pa
Δn	porous thickness, m
FYP	final year project
HVAC	heating, ventilation and air conditioning
HEPA	high-efficiency particulate air
MERV	minimum efficiency reporting value
PSE	particle size efficiency
DHC	dust holding capacity
CFD	computational fluid dynamics
Re	Reynolds number
UPE	ultra-high molecular weight polyethylene
CPU	central processing unit
RAM	random-access memory

LIST OF APPENDICES

CHAPTER 1

INTRODUCTION

1.1   General Introduction

An air filter is a device made of porous materials which removes solid particles such as dust, pollen and bacteria from the air. Air filtration is widely applied in building ventilation systems where air quality is significant. Air filters could improve the breathable environment for the occupants, remove airborne bacteria from the environment, and even minimize the fire hazards by eliminating the flammable particles in the air (EngineerEdge, 2020).

In Heating, Ventilation and Air Conditioning (HVAC) systems, it is generally desirable to remove some of the solid dirt particulates out of the air which is entering the system. The amount of dirt desired to be removed from the incoming air will decide the type of filter media to be used. For instance, a wire mesh screen media could be used to filter large particles adequately, whereas the fine dust must be filtered by fabric materials (Oughton, 2014).

There are few classifications of air filter, such as primary effect air filter, medium effect air filter and high efficiency air filter (Zhang, 2018). Filtration media are often composed of synthetic fibre filters. The outer frame can be made of moisture-proof cardboard, aluminium alloy, galvanised steel, or stainless steel, so it is not easily deformed in the normal operating condition. In addition, it is tightly sealed between the filter media and the frame to prevent air leakage.

The primary effect filter is mainly applied to the primary filtration of HVAC systems, and the pre-filtration of high efficiency air filtration devices. It is commonly used to filter solid particulates with size of 5 µm and above (Zhang, 2018). The filtration media can be made of non-woven fabrics, aluminium wave meshes, nylon netting, aluminium wire meshes, and stainless steel meshes.

High-efficiency particulate air (HEPA) filter is suitable for normal environment condition of temperature and humidity. This type of air filter has high efficiency, but it has high air flow resistance and small dust holding capacity (Zhang, 2018). Due to its high efficiency, it is commonly used in aerospace, pharmacy, semiconductor and biotechnology. For instance, engine air filter is used to protect the mechanical parts of engine by arresting fine solid

particles from the air intake with high efficiency. The cleaner the air intake, the more sustainable is the oil filter element and it can prevent the foreign materials from entering the machine which may cause damage to the machine.

Air flow capacity of the filter is described by the function of the air resistance, as known as the pressure drop of air across the filter media. Conventional HEPA media used glass paper which is composed of large density of micro-fibres to trap micron particles by some mechanical principles. The large density causes restriction to the air flow. Besides, as the micron particles accumulates at the filter media, the filter eventually becomes loaded with dust cake that causes high resistance to the air flow. Hence, the service life expectancy of the filter is usually around 2000 hours, which is equivalent to around 3 months (Zhang, 2018).

In order to prevent large pressure drop caused by high resistance, it is desirable in the case that the area of the filtering media for the air to flow through, is greater than the area of the air inlet of the duct (Debaun, 1966). The practice of pleating increases the area for the air to flow through. Over the years, air filter manufacturers have developed different methods to improve the configurations of the filter media on the pleat shapes and number of pleats per filter to reduce air flow resistance. Figure 1.1 shows the overview design of a pleated air filter and its cross-section. Figure 1.2 shows the schematic drawing of air flows into a pleated filter media in V-shaped made from a flat sheet media.

(1)   (2)
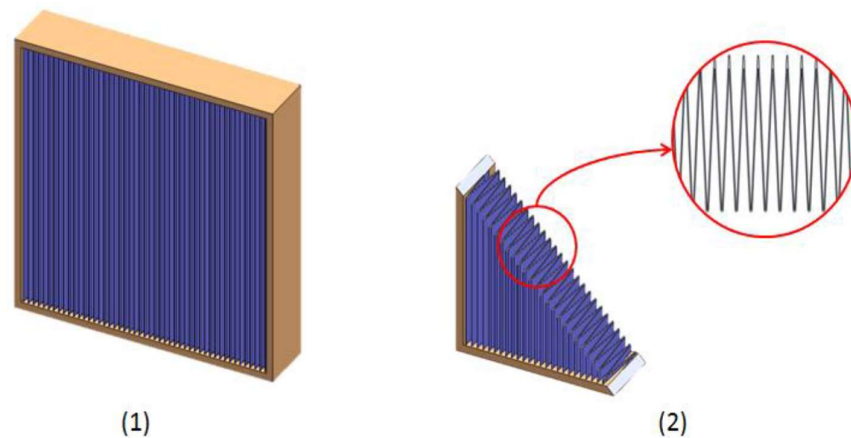
Figure 1.1: Pleated Air Filter. (1) Overview Design of Air Filter and (2) Cross-sectional View of Pleat Design (Schousboe, 2017)
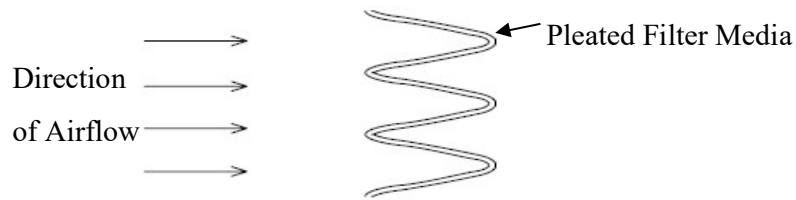
Figure 1.2: Schematic Drawing of Pleated Media (Fu, Fu and Xu, 2014)

1.2 Importance of the Study

Atmospheric air is polluted by various particles, such as ash, pollens, dust, dirt and bacteria. The smallest range of particles to be considered is in the range of 0.01-0.1 μm. This type of particles often found in smoke, cigarette smoke, metal dust and sea salt. Whereas the upper range of particle size to be considered is about 15 μm. These particles are often found in air of fly ash, coal dust, pollen and spores (Oughton, 2014). The removal of larger particles can be done by any mesh of filter with fine aperture to capture the particles. However, the finer the size of the solid particulates to be removed, the finer the aperture of filter media is to capture them, hence leading to high resistance across the air filter media. In air filtration system, one of the most important performance parameters is evaluated by its pressure drop over a range air flow velocity.

In recent development of air filter, the filter media contains large density of randomly oriented fibres and have been folded to form number of pleats (Patil and Lomte, 2015). The thickness of media is often the important influence on the performance of the filter device. Besides, the design of pleat geometry has great influence on the area of air flow through and its flow velocity, which directly affect the pressure drop across the media (Caesar and Schroth, 2002).

Therefore, the study of the geometry and shape of the media pack may lead to significant improvements on the performance of an air filter. In this study, computational fluid dynamics software is used to simulate the flow through the porous filter media, which significantly reduces the experimental work.

1.3 Problem Statement

Pleated filter panels are commonly used to remove solid particulates from the contaminated air because it is more compact and it has larger filtration area compared to a flat sheet media (Chen, Pui and Liu, 1995). The filtration area will vary the media face velocity when the air flows through the filter media,

which affects the residence time of the particles inside the filter media. The key problem in this larger filtration area is whether the change of filtration area will result in improvement on the filter performance and reduce the pressure drop. The area of the filter media must be designed so that the air flow velocity is optimum for the filter to achieve the minimum pressure loss.

One of the methods to increase the filtration area is by increasing the number of pleats. However, if there is excessive pleat number per filter, it will cause failure to the filter by rupturing the filter media (Al-Attar et al., 2010). Therefore, the pleating distance must be optimized to provide the desirable performance at lowest pressure drop. Besides, the height of the pleat also affects the filtration area. Hence, it is desirable as well to consider the pleat height when designing the filter with a given constant pleat distance. Moreover, the shape of the pleat also affects the pressure distribution built inside the pleat. So, it is of interest to compare the influence of geometry of the pleat by its shape such as rectangular or V-shape on the performance of filter media.

In short, these geometrical parameters have significant effects on the performance of an air filter in terms of pressure drop. A key problem in reducing the pressure drop is the influence of interaction among the pleat shape, pleat distance and pleat height. It is desirable to perform simulations to investigate these configurations to achieve the optimum performance of an air filter.

1.4   Aim and Objectives

The main objective of this study is to do investigation on media pack configurations for air filtration devices to improve the performance of the air filter by varying the shape and geometry of the media pack. By characterizing the contributions of a media pack feature on the air filter's overall performance, a systematic approach to design air filters can be developed. The detailed objectives of this project were to:

- Investigate the influence of media pack configuration for an air filter in terms of pleating shape, pleat distance, pleat height of the media pack.
- Use solid modelling computer-aided design software to create models of air filter media with different design of shape and geometry.
- Use computational fluid dynamics software to simulate the flow of the air across the filter media and analyse the pressure drop against velocity.

1.5   Scope and Limitation of the Study

The design scope is on the media pack configuration. The optimization parameters are the pleat shape, pleat distance, and pleat height of the media pack. The influences of these parameters on the pressure drop across filter media were studied. The design was evaluated based on the pressure drop on the filter media at a range of airflow velocity. Optimum results were achieved when the minimum pressure drop was obtained from the interaction between these geometrical parameters.

One of the limitations of the study is that the incoming air was assumed to have uniform velocity profiles. According to Darcy's Law, the incoming air was assumed to be passing through perpendicularly to the filter media surface. The air flowing through the filter media is an incompressible fluid. The filter media is assigned as porous zone with uniform pore size and constant porosity. Furthermore, there were assumptions of neglecting the effects of the developing flow and the permeability at the turning of the pleat.

1.6   Contribution of the Study

The investigation on media pack configurations in this study may help to identify the influence on the performance of air filtration devices in terms of pressure drop across media by making a flat sheet filter media into pleated form. The desirable geometrical design of the pleats for minimum pressure drop can be determined through this study. Moreover, the techniques of using the solid modelling software and the computational fluid dynamics software which were involved in the study may contribute to providing the supporting materials to the future research related to the design of air filtration device.

1.7   Outline of the Report

The report is presented such that Chapter 2 presents an overview of air filtration fundamentals and literature reviews on the pleated filter media. Chapter 3 describes the techniques used to create solid models of air filter and perform simulations. Chapter 4 presents the simulation results and discussion based on detailed analysis. Chapter 5 discusses the conclusion from the current study and recommendations for future study.

CHAPTER 2

LITERATURE REVIEW

2.1 Introduction

The main focus of this study is to investigate the relationship between the configurations of the filter media and the performance of an air filtration device. In order to gain better understanding on the parameters which affect the performance, this chapter focuses on the related research findings from the scientific journals, theoretical and experimental studies and research papers.

2.2 Overview of Air Filter

2.2.1 Air Contaminants

Indoor air pollutants come in various shapes and sizes. There are biological sources like household dust, mould spores, pet's skin cells, bacteria, viruses, tobacco smoke particles and pollens. Generally, the particle shape is assumed to be a spherical model, and the diameter is measured in a metric unit named micron (Oransi, 2020). The metric unit one millimetre is actually equal to 1000 microns, and a micron is approximately 1/25,000 of an inch. Over 20 million particles can be found in the average cubic foot of indoor air and approximately 98 % of the particles are in the size of 5 microns or less (Dynamic Air Quality Solutions, 2020). Figure 2.1 shows the range of size of the common pollutants.
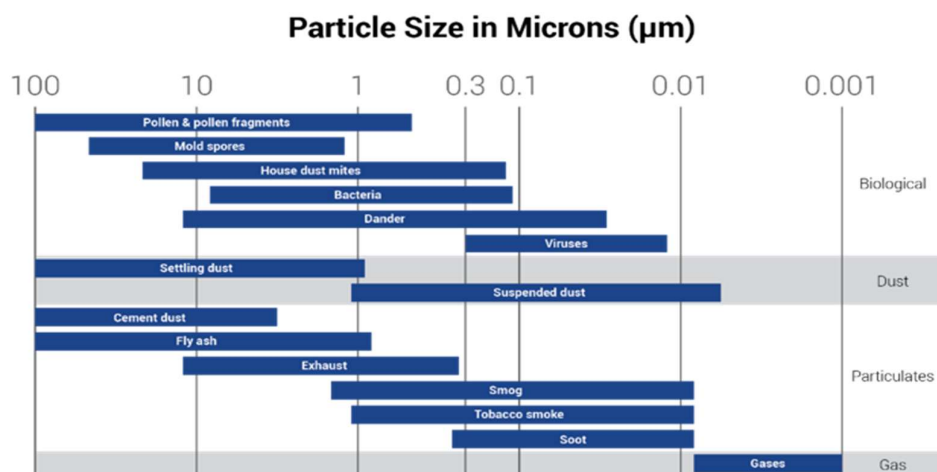
Figure 2.1: Size Range Chart of Common Pollutants (Kelley, 2019)

2.2.2 Indoor Air Quality (IAQ)

ANSI/ASHRAE Standard 52.2 was developed in 1999. ASHRAE Standard 52.2-2017 is the updated publication, which provides a method to determine the efficiency of a filter in removing different sized of particles when the filter becomes loaded and measure the resistance of the filter to airflow when clean. The efficiency of the filter is calculated by determining the number of upstream and downstream particles through a range of particle sizes. Then, the evaluated air filter is reported with a single number expressed as the Minimum Efficiency Reporting Value (MERV). There are twelve ranges of particles placed in three larger groups: E1 (range 1-4), E2 (range 5-8) and E3 (range 9-12). Composite Minimum Efficiency is averaged for each of these groups to calculate the average Particle Size Efficiency (PSE), which is then used to determine MERV (AAF, 2017). The higher the MERV, the more effective it is at filtering the finest particles. Table 2.1 shows the ranges of particle size are divided into three groups. Table 2.2 shows the MERV Parameters Table.

Table 2.1: ANSI/ASHRAE 52.2 Particle Size Range in μm (AAF, 2017)

Range	Size	Group
1	0.30 to 0.40	E1
2	0.40 to 0.55	E1
3	0.55 to 0.70	E1
4	0.70 to 1.00	E1
5	1.00 to 1.30	E2
6	1.30 to 1.60	E2
7	1.60 to 2.20	E2
8	2.20 to 3.00	E2
9	3.00 to 4.00	E3
10	4.00 to 5.50	E3
11	5.50 to 7.00	E3
12	7.00 to 10.00	E3

Table 2.2: MERV Parameters Table (AAF, 2017)

Standard 52.2 Minimum Efficiency Reporting Value (MERV)	Composite Average Particle Size Efficiency, % in Size Range, μm			Average Arrestance, %
	Range 1 0.30-1.0	Range 2 1.0-3.0	Range 3 3.0-10.0	
1	N/A	N/A	$E_3 < 20$	$A_{avg} < 65$
2	N/A	N/A	$E_3 < 20$	$65 \leq A_{avg}$
3	N/A	N/A	$E_3 < 20$	$70 \leq A_{avg}$
4	N/A	N/A	$E_3 < 20$	$75 \leq A_{avg}$
5	N/A	N/A	$20 \leq E_3$	N/A
6	N/A	N/A	$35 \leq E_3$	N/A
7	N/A	N/A	$50 \leq E_3$	N/A
8	N/A	$20 \leq E_2$	$70 \leq E_3$	N/A
9	N/A	$35 \leq E_2$	$75 \leq E_3$	N/A
10	N/A	$50 \leq E_2$	$80 \leq E_3$	N/A
11	$20 \leq E_1$	$65 \leq E_2$	$85 \leq E_3$	N/A
12	$35 \leq E_1$	$80 \leq E_2$	$90 \leq E_3$	N/A
13	$50 \leq E_1$	$85 \leq E_2$	$90 \leq E_3$	N/A
14	$75 \leq E_1$	$90 \leq E_2$	$95 \leq E_3$	N/A
15	$85 \leq E_1$	$90 \leq E_2$	$95 \leq E_3$	N/A
16	$95 \leq E_1$	$95 \leq E_2$	$95 \leq E_3$	N/A

2.2.3   Mechanism of Filtration

The ability of filter to remove solid particles is dependent on various types of mechanisms. The significance of these mechanisms depends on the required efficiency of the filter. Generally, an air filter is often designed to employ a combination of mechanisms to capture the particles from the air. Each mechanism of filtration, including diffusion, interception, inertial impaction and sieving, is used to remove specific range of particle sizes. For instance, sieving, interception and inertial impaction are employed for particle size greater than 0.2 microns, whereas diffusion is employed for particle smaller than 0.2 microns (Air Quality Engineering, 2018). Figure 2.2 shows the schematic drawing of the filtration processes happen in the filter media.
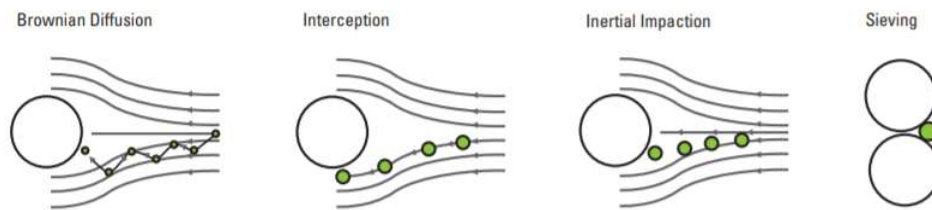
Figure 2.2: Filtration Mechanism (Sipes, 2011)

Mechanical sieving occurs where the diameter of the solid particles is larger than the opening between the filter media materials. As the opening must be smaller than the size of the particle, it will cause higher pressure-drop and lower dust holding capacity. Therefore, this mechanism is only suitable to remove large particles.

Inertial impaction happens when large particles travels on their original straight path initially, then collides with the fibre and remains there. This is because large particles have high momentum, so their path will not be affected by the air flow. The greater the air velocity, the greater the inertial effects.

Interception occurs when the particle travelling in a straight line makes contact with a fibre in the filter and then attached to the media. The particulate is smaller, normally 1-5 μm, and its inertia is not strong enough to travel in a straight line steadily, plus the density of the fibres in the media is high (Air Quality Engineering, 2018). Therefore, the particle follows the air stream around the fibre until it comes close enough to the fibre and collides with it.

Brownian diffusion occurs when the Brownian motion of a particle has caused it to make contact with a fibre by molecular force. This mechanism only occurs in very small particles, <0.5 μm approximately (Oughton, 2014). The type of filter which employs this mechanism is the high-efficiency particulate air (HEPA) filter. The efficiency of this type mechanism depends on maximizing the time of contact between the particles and the filter media. The greater the filtration area, the more time the particle is in the media, hence the higher the chances of removal.

Electrostatic removal happens when the air flowing through the filter media and generate an electrostatic charge on the media. The charge will attract the particles to the fibres and attached to it. Typical media are polyester and polypropylene (Oughton, 2014).

2.2.4   Types of Air Filter Materials

Air filter material is the filtering component in the air filters. The type of material is selected based on the application of the air filter. Generally, there are many different types of materials can be selected to design the type of air filter depends on the types of particulates to be removed.

One of the most reliable materials for dust removal is spun fiberglass. Fiberglass is good at trapping large particles, such as dust and animal dander. In air filtration industry, most of the HEPA filters are made from fiberglass. Compared to other types of materials, fiberglass filters are more affordable. However, the fiberglass filter requires more filter media, so the pressure drop will be higher (Oransi, 2020).

The next material is activated carbon. Activated carbon is made from charcoal. However, carbon must be treated with heat, chemicals and other methods, so that this highly porous materials is activated to remove various tiny contaminants, including those which are too small for HEPA filters.

There is one type of plastics material, polypropylene, which is durable, reliable and washable. This synthetic filter can be effective resources for removing impurities in the air through a combination of air flow and electrostatic charge. The electrostatic charge is created by the friction of air flow over the air filter woven surface. The woven polypropylene media has excellent strength and high resistant to abrasion, acids and alkali (Permatron, 2020).

2.3   The Importance of Pleated Air Filters

A pleated air filter is made by folding the filter media into pleats to increase the entire surface area. The greater filtration area means that it has more material to trap more particles. In air filtration, the effective filter media area is a significant characteristic of an air filter. Effective filter area is defined as the medium area which air passes through (EMW, 2020). EMW conducted an investigation to compare between the two air filtration devices with different effective filter area. Figure 2.3 shows the comparison between 25.3 m^2 area of MPK 412-31 GT and 30.5 m^2 area of MPK 412-38 GT. Results show that for particle size smaller than 0.3 µm, the decreased effective area does cause a drop in filter efficiency.
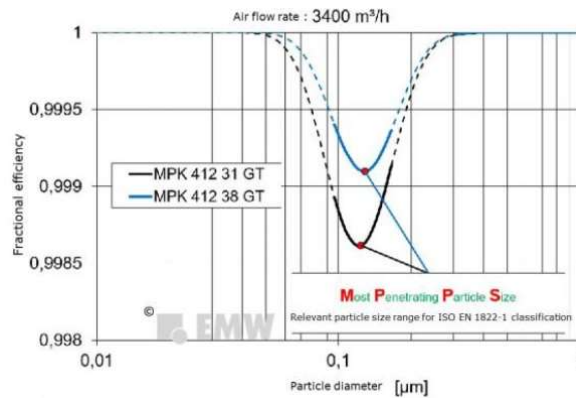
Figure 2.3: Fractional Efficiency Against Particle Diameter (EMW, 2020)

The geometry of pleated air filter is illustrated in Figure 2.4. V is the face velocity; Y is the pleat distance or pleat pitch; L is the pleat height or pleat depth; s is the thickness of filter media; and $H(x)$ is the distance between the pleats from x. Theoretically, there are some assumptions made to analyse the performance of the pleating air filter, including the incompressibility of air, which the air density and air dynamic viscosity are constant, and no external force acted at x direction (Fu, Fu and Xu, 2014).
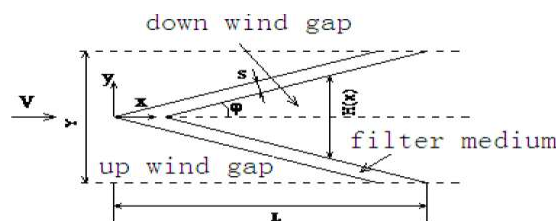
Figure 2.4: Schematic Geometry of Pleated Air Filter (Fu, Fu and Xu, 2014)

The effective filtration area is actually influenced by the pleat geometry. Pleat density is defined as the number of pleats per width of filter media, which is varied by the distance between the pleats. An experimental work involved the testing of pleated air filter was performed by Al-Attar et al. (2010), which used four filters manufactured by EMW with pleat density ranging from 28 to 34 pleats per 100 mm. The effective filtration area increased with the pleat density as shown in Table 2.3. However, it was mentioned that over-pleating will cause failure due to large pressure drop. Consequently, the pleat geometry must be optimized to obtain the desirable efficiency at minimum pressure drop.

Table 2.3: Pleat Density and Surface Area of EMW Filters (Al-Attar et al., 2010)

Pleat Density (pleats/100 mm)	Surface Area (m^2)
28	23.9
30	26.6
32	27.3
34	28.9

2.4   The Influence of Pleat Geometry

In air filtration devices, the pressure drop across the filter media is an important parameter of the performance of an air filter. Caesar and Schroth (2002) investigated the variation of pressure drop caused by the pleating geometry in deep-pleated cassette filters by using Navier-Stokes equation for stationary flows. Figure 2.5 shows a filter media pleated in V-shaped geometry. The air flows to the pleats at the velocity $\bar{w}_\infty$, and enters the pleats at $z = 0$. Due to the V-shaped geometry, the flow sectional area becomes narrow, which causes the air to accelerate. The air passes through the filter medium at velocity $v_M(z)$. Then, it exits to the surrounding at $z = F_T$ at lower velocity because the flow sectional area has become widen. Caesar and Schroth stated that there are three components contributing to the total pressure drop, including the pressure drop by friction loss inside the pleat, pressure drop at the narrowing and widening of flow sectional area, and pressure drop by the filter medium. Figure 2.6 shows the rectangular pleated media.
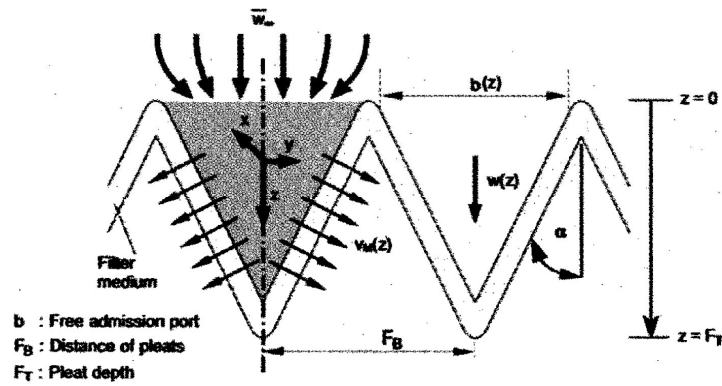
Figure 2.5: V-shaped Pleated Filter Medium (Caesar and Schroth, 2002)
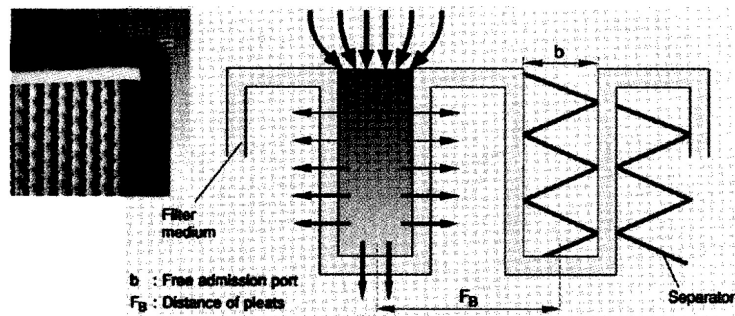
Figure 2.6: Rectangular Pleated Filter Medium with Separators (Caesar and Schroth, 2002)

In the study, the pressure drop between the V-shaped and rectangular pleat geometries were compared. Figure 2.7 shows the results of comparison that V-shaped pleating causes lower pressure drop than the rectangular pleating. This is due to the fact that pressure distribution built up in the rectangular pleats, causing the air to flow through the media faster at the bottom than the upper part. Due to the uneven flow on the media, the pressure drop is therefore increased in rectangular pleats. Whereas in V-shaped pleating system, the air flows through the medium at the same angle of direction, thus uniform pressure applied over the filter area. The resistance is applied evenly in the V-shaped pleated media.

It was also found that the pressure drop can be affected by various pleat depths, pleat distances and face velocities. Figure 2.7 also shows that the reduce in pleat distance will reduce the pressure drop due to increase in filter area. But after a certain distance, the increase of area will lead to rise of pressure drop. Therefore, a large area could not be always advantageous. Eventually, there is an optimum pleat distance for each type of filter media.
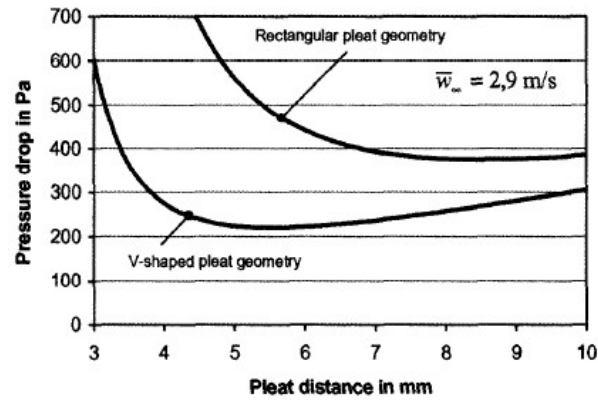
Figure 2.7: Pressure Drop for V-shaped and Rectangular Pleated Filter Media with Various Pleat Distances (Caesar and Schroth, 2002)

Besides, Figure 2.8 shows that given constant pleat distance and pleat depth, the pressure difference increases with the rise of face velocity as well. When the air flows through the pleat depth 280 mm media, the pressure drop at the face velocity 2.9 ms^{-1} is higher than at 1.0 ms^{-1}.
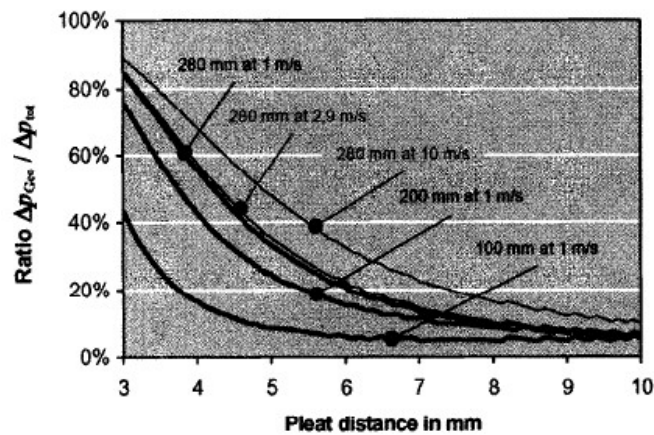
Figure 2.8: Pressure drop caused by different pleat depths and face velocity (Caesar and Schroth, 2002)

Maddineni, Das and Damodaran (2019) investigated the pressure difference in the pleated air filter system through numerical simulations and laboratory experiments. The pressure drop characteristics were obtained by using the pleated filter element of various pleat pitch and pleat height. The study had found that at the optimal pleat pitch and pleat height, the lowest pressure drop was obtained.

Figure 2.9 shows the results obtained from experiments and simulations. The pressure drop first reduced with the increasing pleat pitch until an optimal point, then followed by increased pressure drop. Initially, the decrease in pressure drop with the increasing pleat pitch before the optimal point is caused by the widen of pleat channel, so the air drag force due to inertial effects had been weakened. Then, when the pleat pitch increased more than optimal point, the effective filter area had been decreased, so it led to the pressure drop across the filter media start to increase. Thus, the optimum pitch is the best trade-off between the air drag effect and low filtration area.

Besides, the results showed that the optimal pitch value was shifted to the higher value when the pleat height increased. Hence, it is clear that the interaction between the pleat pitch and pleat height does affect the optimal pressure drop due to the effective filer area. Figure 2.10 shows that the increase of pressure drop was much significant with the increasing inlet velocity.
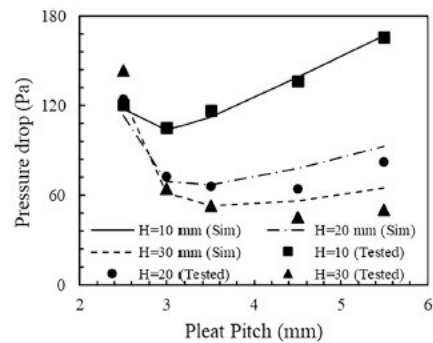
Figure 2.9: Pressure drop against pleat pitch at various pleat heights (Maddineni, Das and Damodaran, 2019)
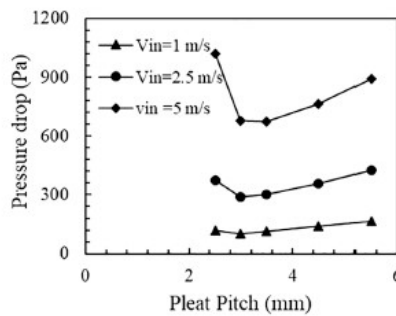
Figure 2.10: Pressure drop against pleat pitch at various inlet velocities (Maddineni, Das and Damodaran, 2019)

Chen, Pui and Liu (1995) developed a finite element numerical model to optimize the pleated filter designs. The numerical results were used to compare with the experimental results obtained in previous study done by Yu and Goulding (1992). In this study, the numerical model has involved all the influence caused by the development of flow, flow contraction and expansion, which had not been considered in the previous study. An analysis of the velocity field in a rectangular pleated had been done. By referring to Figure 2.11, the inlet velocity seems to increase when the fluid flow is approaching the pleated media. The flow seems to contract at the filter region, where major flow enters the upstream pleat channel and becomes fully developed shortly, while minor flow passes through the media directly. When leaving the filter media, the minor flow will then enter the downstream pleat channel and becomes fully developed shortly, while the major flow will go through the media. Then, the velocity distribution will be recovered to uniform profile.
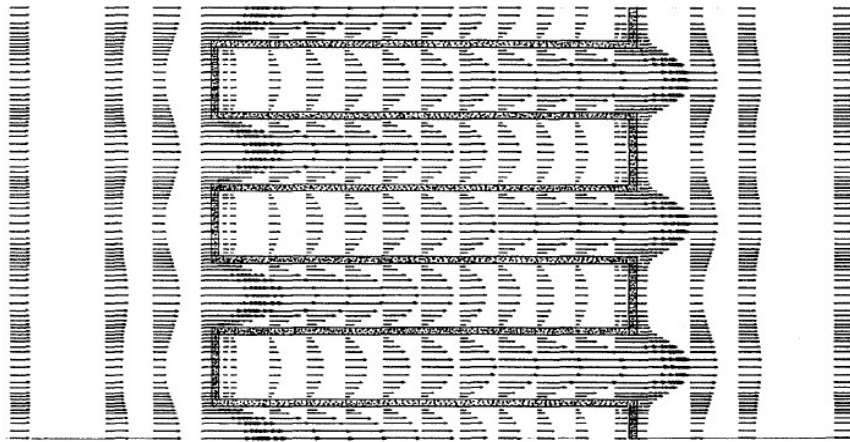
Figure 2.11: Velocity profile of rectangular pleated air filter (Chen, Pui and Liu, 1995)

The numerical model also includes the optimization of pressure drop. In Figure 2.12, the pressure drop is shown as a result of varying the pleat count and pleat height for the filter media, and the result is compared with those of Yu and Goulding. The pressure drop rises at low pleats because low filtration area causes the media face velocity increased. When there are too many pleats, the pressure drop rises again because the viscous drag effect is has become more significant.
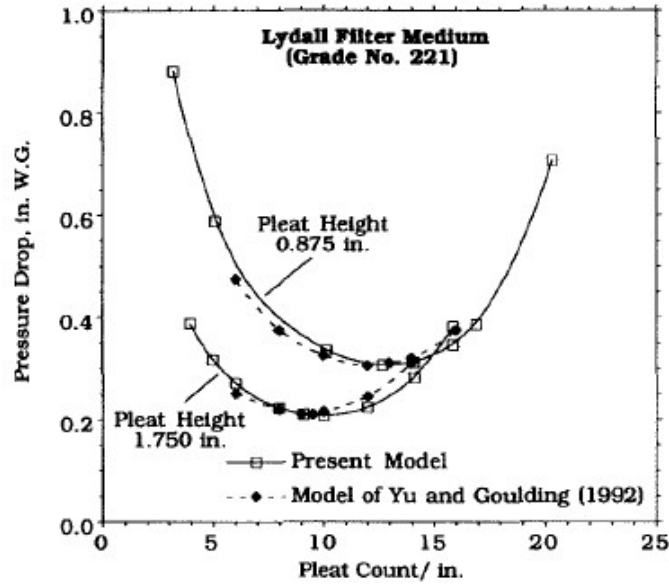
Figure 2.12: Pressure drop against pleat count (Chen, Pui and Liu, 1995)

When comparison, this study had found that at smaller pleat count, the pressure drop of Yu and Goulding's results are lower than numerical result, but at higher pleat count, the pressure drop becomes larger than numerical result. The discrepancy is because Yu and Goulding had neglected the flow contraction and expansion. The numerical model also shows that when comparison is made between filters with constant pleat heights, the lowest pressure drop is obtained when an optimal pleat count is obtained.

2.5   Summary

This literature review provides the overview of air filtration fundamentals, including the types and ranges of size of the particles to be removed by air filtration devices, and the standard which commonly used to rate the efficiency of the filter to trap the particles in different range of size. It also explains the theory of air filtration mechanism and the common types of materials used in air filter media.

Based on this literature review, the importance of the pleating feature on the air filter media to increase the effective filter area was determined. Besides, it also helps in providing a better understanding on the optimization parameters, such as pleat shape, pleat height, and pleat distance or pleat density to improve the performance of the air filter devices in terms of pressure drop across media.

CHAPTER 3

METHODOLOGY AND WORK PLAN

3.1 Introduction

The project was started by identifying the problem statement, followed by the formulation of the aim and objective. Literature review in Chapter 2 was performed to obtain information from the related research. Methodology was described in Chapter 3, which involves the design phase and simulation phase. The obtained results were analysed and discussed in Chapter 4. Chapter 5 presents the conclusion and recommendation for this project. The work plan for the entire project is presented in Figure 3.1.
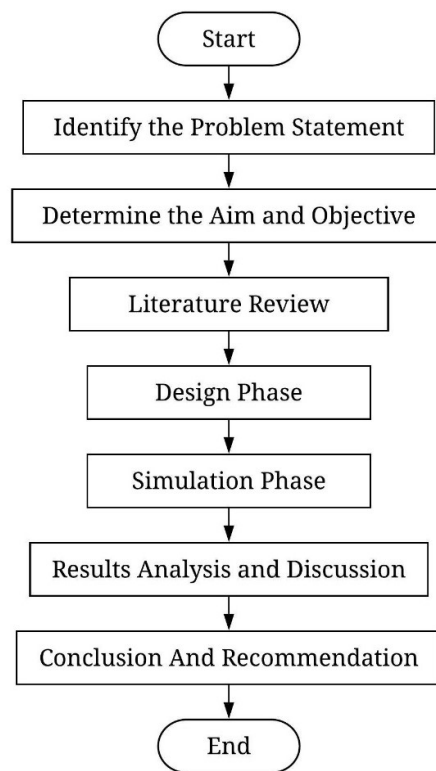
Figure 3.1: Flow Chart of the Project

3.2   Work Plan

The project is assigned to be completed in two semesters. Hence, the project is split into two parts, which are the Part 1 and Part 2. Project Part 1 was started with planning activities, including identification of problem statement and formulation of aim and objective for one week. Literature review was performed on related research for six weeks. Research methodology had been identified for the design phase and simulation phase. 3D modelling and simulation were done in six weeks as well by using Solidworks and ANSYS Fluent software to obtain the preliminary results. The compilation of progress report was completed in two weeks, followed by report submission and presentation in the final week of the semester. Figure 3.2 shows the Gantt Chart for Project Part 1.

Project Activities	W1	W2	W3	W4	W5	W6	W7	W8	W9	W10	W11	W12	W13	W14
Project Planning	█													
Literature Review		█	█	█	█	█	█							
Design Phase & Simulation							█	█	█	█	█	█		
Report Writing												█	█	
Report Submission & Presentation														█

Figure 3.2: Work Plan of Project Part 1

After identifying and analysing the preliminary results in Project Part 1, the selected input parameters in the geometrical modelling and the conditions in simulations were carried to the next part. Project Part 2 was started with the 3D design of air filtration media. Solidworks was used to create different designs of the filter media by varying the configurations of the media such as the pleat shape, pleat distance, and pleat depth. The design process took four weeks to be completed. At the middle of 3D modelling process, the design was analysed by using Ansys Fluent to simulate air flow through the filter media. The simulation was performed on a single pleat in 2D body to improve efficiency of simulation because most of the parts on the filter media are symmetrical to each other. From Week 7 onwards, the output of the simulations was tabulated and inserted into

the final report. At the same time, discussions were made based on the analysis of the results. At Week 12, the discussions were completed and the FYP Poster was submitted. After that, the FYP final report and FYP presentation slides were completed by using two weeks' time. Submission of FYP final report and the Project Part 2 presentation were done in the final week. Figure 3.3 shows the Gantt Chart for Project Part 2.

Project Activities	W1	W2	W3	W4	W5	W6	W7	W8	W9	W10	W11	W12	W13	W14
Design of Air Filtration Media	███	███	███	███										
CFD Simulation			███	███	███	███	███	███						
Result and Discussion							███	███	███	███	███	███		
Report Submission & Presentation												███	███	███

Figure 3.3: Work Plan of Project Part 2

3.3 Flat Sheet Filter Media

The property of flat sheet media was obtained from the property sheet of a filter media produced by Lydall Performance Materials, a leader in innovative filtration industry. The high-performance filter media, named Arioso, is designed to combine high filtration efficiencies and extremely low pressure drop. The Arioso media is made from ultra-high molecular weight polyethylene (UPE) and laminated to glass fibers as support layer to form mechanically robust composite. Figure 3.4 shows the air filtration properties of Arioso media, while Figure 3.5 shows the physical properties of Arioso media. Figure 3.6 shows the graph of resistance against airflow velocity. In the stage of simulation phase, the filter media was treated as porous zone, and the relationship between the pressure drop and airflow velocity was studied to check the validity of the simulation results.

Typical Air Filtration Properties (TSI Model 3160 CNC)					
Typical Properties	US Customary Units		SI Units		Reference Test Methods
Filter Class	MERV 15/16	ASHRAE 52.2	F9	EN779	Flat Sheet
Efficiency (0.3μm DEHS @ 5.33 cm/s)	95.4	%	95.4	%	MIL-STD-282 A.S.T.M. - D2986-91
Penetration (0.3μm DEHS @ 5.33 cm/s)	4.6	%	4.6	%	MIL-STD-282 A.S.T.M. - D2986-91
MPPS Efficiency (0.3μm DEHS @ 5.33 cm/s)	87.5	%	87.5	%	MIL-STD-282 A.S.T.M. - D2986-91
MPPS Penetration (0.3μm DEHS @ 5.33 cm/s)	12.5	%	12.5	%	MIL-STD-282 A.S.T.M. - D2986-91
Air Resistance (5.33 cm/s)	4.6	mm H_2O	45	Pa	MIL-STD-282 A.S.T.M. - D2986-91
Air Permeability/Frazier (125 Pa)	33	ft³/ft²/min	16.8	cm³/cm²/s	TAPPI T - 251

Figure 3.4: Air Filtration Properties of Arioso (Lydall, 2016)

Typical Physical Properties of *Arioso*® Composite					
Typical Properties	US Customary Units		SI Units		Reference Test Methods
Functional Support Layer	Glass, Wet-Laid		Glass, Wet-Laid		
Basis Weight	34.1	lbs/3000 ft²	55	g/m²	T.A.P.P.I - T - 410 A.S.T.M. - D -646
Gurley Stiffness (MD)	650	mgf	650	mgf	T.A.P.P.I. - T - 543
Thickness/Caliper (7.3psi / 50 kPa)	13.6	mils	0.34	mm	T.A.P.P.I. - T - 411
Water Repellency	28	in. wg	711	mm wg	MIL STD 282
Continuous Operating Temperature	176	°F	80	°C	Max

Figure 3.5: Physical properties of Arioso (Lydall, 2016)
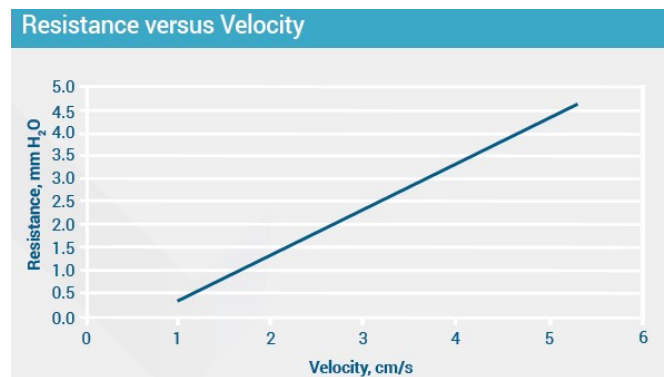
Figure 3.6: Resistance versus Velocity (Lydall, 2016)

3.3.1 Modelling the Porous Media

In this study, the filter media is treated as a porous medium in CFD simulation. When a porous media model is applied, the pressure drop in the flow can be obtained through the momentum equation. The porous media are constructed by the insert of source term of momentum equation into standard fluid flow equations. For the case of simple homogeneous porous media, the source term, S_i for the ith momentum equation is determined by using Equation 3.1.

$$S_i = - \left(\frac{\mu}{\alpha} V_i + C_2 \frac{1}{2} \rho |V| V_i \right)$$

(3.1)

where

α = permeability, m^2

V = magnitude of the velocity, m/s

ρ = density of fluid, kg/m^3

μ = dynamic viscosity, kg/(m $\cdot$ s)

C_2 = inertial resistance factor, m^{-1}

When the momentum equation is simplified, the pressure drop can be related to the source term, S_i and expressed as Equation 3.2.

$$\Delta p = -S_i \Delta n$$

(3.2)

where

Δp = pressure drop, Pa

Δn = thickness of the porous media, m

However, when the fluid is flowing through the porous media in laminar flow, the pressure drop is directly proportional to the velocity, so the constant inertial resistance factor C_2 is considered as zero. Hence, the porous model can be simplified to Darcy's Law in Equation 3.3.

$$\Delta p = \frac{\mu}{\alpha} V \Delta n$$

(3.3)

where

Δp = pressure drop, Pa

μ = dynamic viscosity, kg/(m · s)

α = permeability, m^2

V = magnitude of the velocity, m/s

Δn = thickness of the porous media, m

3.4 Design Phase

This section mainly focuses on the modelling of filter media. First, the design of the air filtration device was determined by taking a filtration product from a manufacturer as a reference to initialize the design. Alternative designs were created by varying the configurations of the pleat geometry in terms of pleat shape, pleat distance, and pleat height based on the findings in literature review. The 3D model of the air filtration devices was generated by using Solidworks.

3.4.1 External Dimensions of Air Filtration Device

The design of the air filtration device was determined based on a property sheet of a commercially available air filter. "Absolute Filter THINFIL Minipleat" is a HEPA filter device made by Cambridge Filter Corporation. Based on the property sheet, the external dimensions of model "1T-600" are 610 mm in height and 610 mm in width (Cambridge Filter Corporation, 2006). Figure 3.7 shows the mini-pleat HEPA filter of Cambridge Filter Corporation.

Figure 3.7: Absolute Filter THINFIL Minipleat (Cambridge Filter Corporation, 2006)

3.4.2   Model Pleat Shape

Two different types of pleat shape were considered in the design of filter media, including V-shaped pleat and rectangular pleat. The purpose is to investigate the influence of making the flat sheet filter media into pleated shape. The effects of both shaped on the pressure drop were determined as well to specify the best pleat shape which reduced the pressure drop the most. Figure 3.8 shows the cross-section of both V-shaped pleat and rectangular pleat.
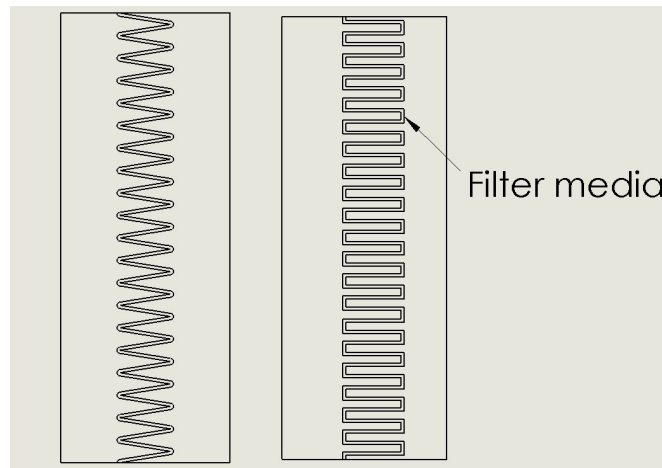
Figure 3.8: V-shaped Pleat (Left) and Rectangular Pleat (Right)

3.4.3   Pleat Distance

In this study, a range of pleat distance from 1.5 mm to 6 mm was suggested to investigate the impact of various pleat distance on the pressure drop through the pleated filter media. This range of pleat distance was actually determined based on the pervious study made by Tronville and Sala (2003). Figure 3.9 shows the rectangular pleats with two different pleat distances.
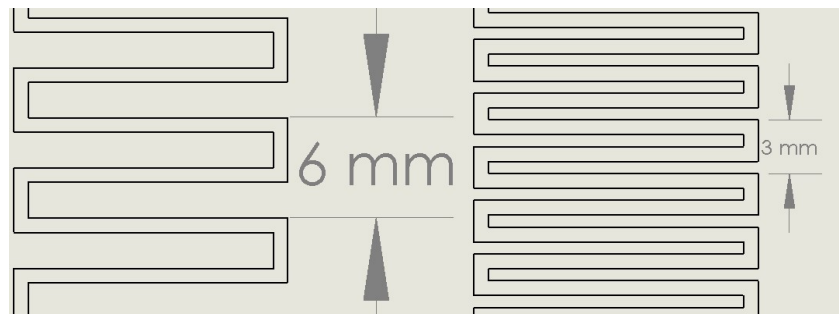
Figure 3.9: Rectangular Pleats Distance at 6 mm (Left) and 3 mm (Right)

3.4.4   Pleat Height

Two different pleat height of 25 mm and 35 mm were suggested based on the research conducted by Allam and Elsaid (2020). The purpose is to study the influence of two different pleat height on the pressure drop through the pleated filter media with similar pleat shape and pleat distance. Figure 3.10 shows the rectangular pleated media with two different pleat height of 25 mm and 35 mm.
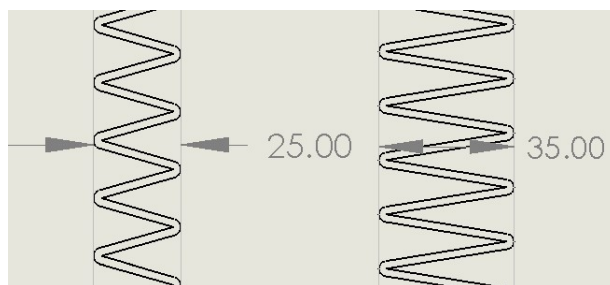
Figure 3.10: V-shaped Pleat Heights at 25 mm (Left) and 35 mm (Right)

3.4.5   3D Modelling

The geometrical parameters in terms of the pleating configurations were tabulated as shown in Table 3.1 and labelled in Figure 3.11.

Table 3.1: Geometrical Parameters of the Pleated Air Filter

Geometrical Parameters	Pleat Configurations
Pleat Shape	V-Shaped and Rectangular Shape
Pleat Distance, Y	From 1.5 mm to 6 mm
Pleat Height, L	25 mm and 35 mm
Thickness of media, S	0.34 mm
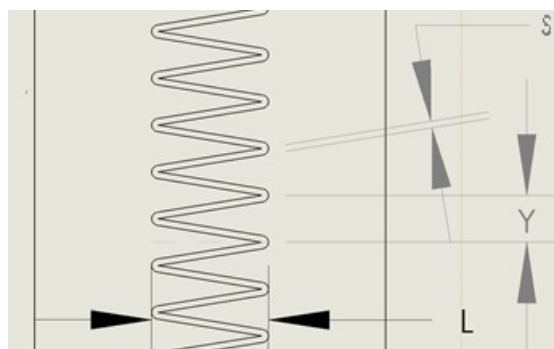
Figure 3.11: Label of Geometrical Parameters on Pleated Filter Media

By using the combinations of geometrical parameters, different types of 3D models were constructed by using Solidworks software. This step is to apply the pleat configurations into the 3D model to check the validity of the design of pleated filter before proceeding to the simulation phase. Figure 3.12 shows the V-shaped pleated media with pleat distance of 3 mm and pleat height of 25 mm, while Figure 3.13 shows rectangular pleated media with pleat distance of 6 mm and pleat height of 35 mm.
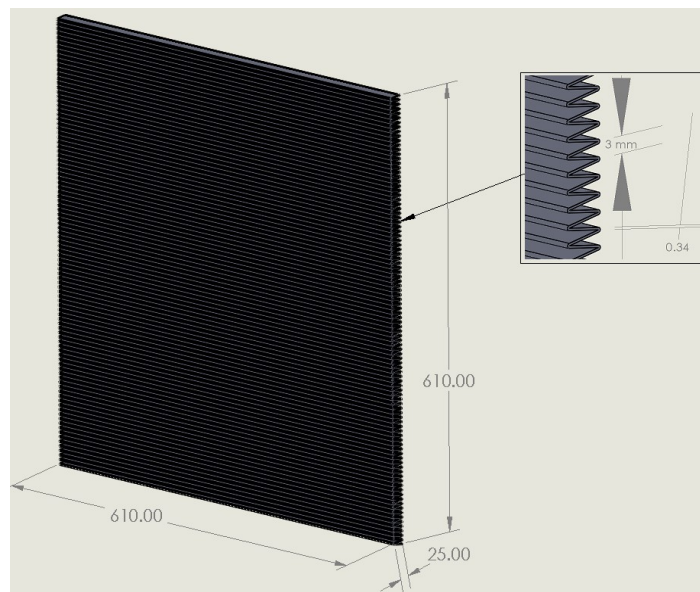
Figure 3.12: V-shaped Pleated Air Filter Media
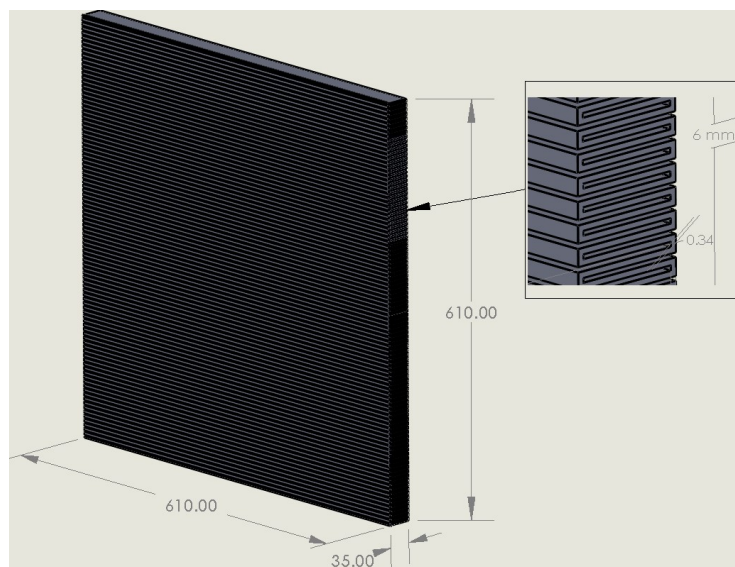
Figure 3.13: Rectangular Pleated Air Filter Media.

3.5   Simulation Phase

This section describes the steps of computational fluid dynamics simulation in Ansys Fluent Software. First, 2D geometry of the air filter media was created. Meshing on the body was performed with inspection on the grid independence. The simulation of the flow through porous media was solved with the defined boundary conditions and cell zone conditions. Results were generated based on the computational calculations.

3.5.1   Geometry

Ansys DesignModeler was used to create the 2D geometry of the air filter media with the pleating configurations as designed in Chapter 3.4. In this study, the application of 2D geometry to represent the 3D model is due to the similarity of the cross section across the whole body of filter media. In addition, a single pleat was generated instead of multiple pleats due to the similarity of pleat geometry on the media, hence the pleat geometry can be developed as asymmetry domain. Therefore, the computational domain of the pleated air filter used in this study was simplified as shown in Figure 3.14 and Figure 3.15. Different types of pleat geometry were created by varying the parameters such as pleat shape between V-shaped and rectangular shape, a range of pleat distance from 1.5 mm to 6 mm, and pleat height of 25 mm and 35 mm. In addition, body of fluid was generated as well to surround the filter media for simulation of fluid flow.
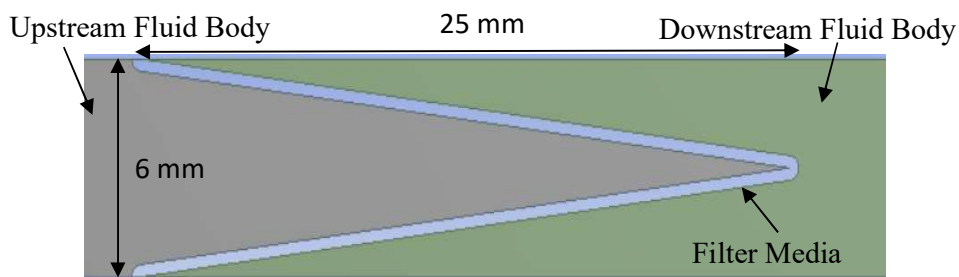
Figure 3.14: V-shaped Pleat at 6 mm Pleat Distance and 25 mm Pleat Height
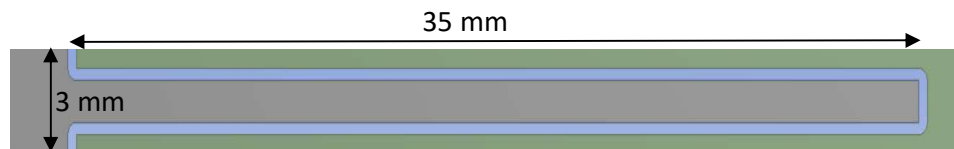
Figure 3.15: Rectangle Pleat at 3 mm Pleat Distance and 35 mm Pleat Height

3.5.2 Mesh

Meshing was used to divide the geometry into simple elements for local approximations of the larger domain. This subchapter involves the meshing method, element sizing, and named selections part.

Figure 3.16 shows the V-shaped pleated filter media and the body of surrounding fluid were meshed. MultiZone mesh method was applied with mesh type of quadrilateral and triangular element (Quad/Tri). The use of multizone meshing enables the triangles for better quality and transitioning.
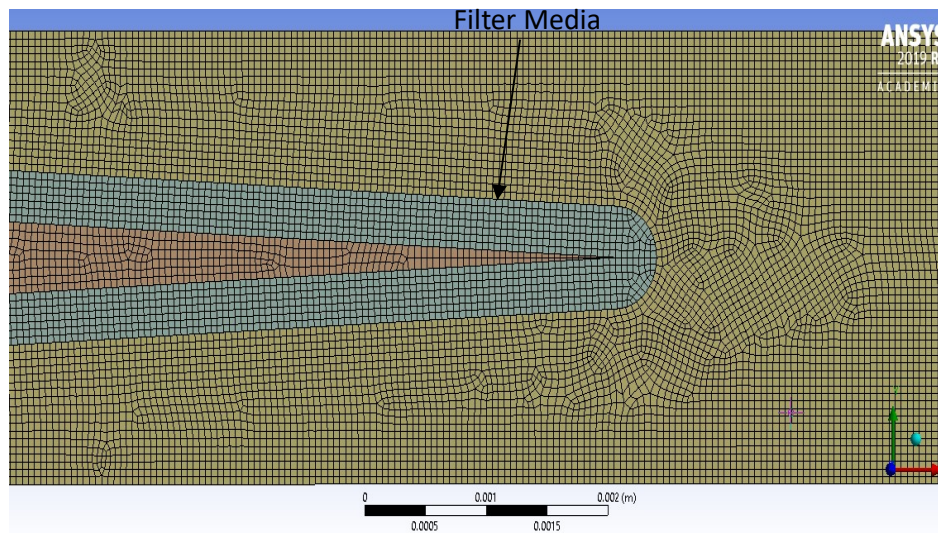
Figure 3.16: Zoomed-in View of Meshes on Filter Media

Face Sizing was used to add a sizing to the entire surface of filter media and fluid based on the element size. The element size specifies the average length of the elements' edges on the bodies. Hard behaviour meshing was set so that the element size produced as per input size. In order to check the validity of element size, the mesh size was varied from coarse to fine and the output result for each was checked. In this study, the generated model was meshed with eight sets of grid size ranging from 0.03 mm to 0.2 mm. The pressure drop across the filter media was selected as the output result. Then, the relationship between the output result and mesh density was studied by plotting a graph. The mesh size was said to be preferred for computation when the output result does not change much with the element size, so that the accuracy of the results is guaranteed.

3.5.3   Setup

This subchapter is the most significant part for the simulation, as it involves the input parameter to set the initial conditions. The setup was started with pressure-based type of solver, absolute velocity formation, and steady analysis, where the result will be obtained at infinite time.

3.5.4   Models

The Reynolds Number (Re) is a non-dimensional parameter to indicate whether the flow of the fluid in laminar or turbulent. It is considered that the flow is laminar when the Reynolds Number is smaller than 2300. The flow is in transition between laminar to turbulent when the Reynolds Number is between 2300 and 4000. Turbulent flow occurs if the Reynolds Number is greater than 4000 (Cengel and Cimbala, 2012). The Reynolds Number is defined as stated in Equation 3.4.

$$Re = \frac{\rho V D}{\mu}$$

(3.4)

where

ρ = density of fluid, kg/m^3

V = flow velocity of fluid, ms^{-1}

D = hydraulic diameter, m

μ = dynamic viscosity, kg/ms

In the case of square duct in this study, the hydraulic diameter is obtained by Equation 3.5.

$$D = \frac{4A}{P}$$

(3.5)

where

A = area of the duct, m^2

P = perimeter of the duct, m

By solving Equation 3.5, the hydraulic diameter of the duct can be obtained. The hydraulic diameter was applied to determine the Reynolds Number of the flow. Hence, the type of the fluid flow can be determined. If the flow is laminar model, the viscous model setting will be set at Laminar. Whereas the viscous model setting will be set at the Reynolds stress model (RSM) turbulence model. RSM is more preferable than the k-ε standard model and renormalization group (RNG) k-ε model due to better convergence (Tronville and Sala, 2003). By solving the Equation 3.4 and the Equation 3.5 with the width and the height at 0.61 m, the hydraulic diameter, $D = 0.61$ m, the density and viscosity of air at 25 °C, $\rho = 1.184$ kg/m^3 and $\mu = 1.849 \times 10^{-5}$ kg/(m $\cdot$ s) respectively, and the face velocity is set at 0.0533 m/s as shown in Figure 3.4 for simulation on flat sheet media, the Reynolds number is determined to be 1343, which is smaller than 2300. Therefore, it is laminar flow. When the velocity increases, Reynolds number increases to become turbulent model eventually. Figure 3.17 shows the viscous model as laminar and RMS.
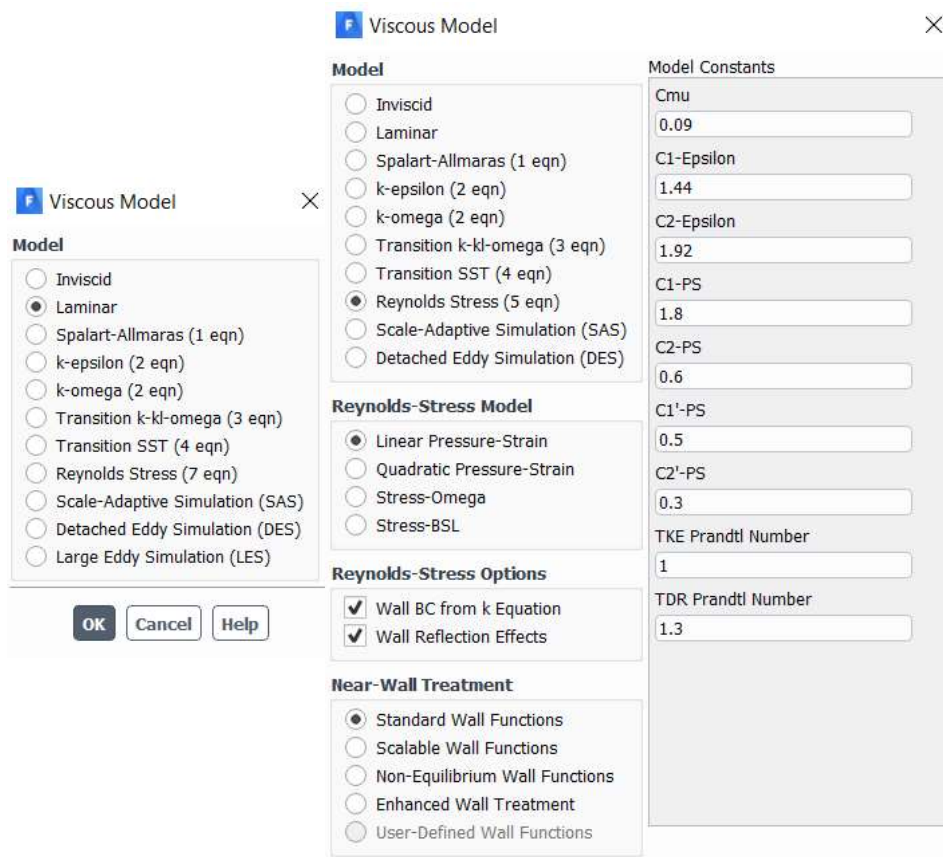
Figure 3.17: Laminar Model (Left) and Reynold Stress model (Right)

3.5.5 Materials

The simulation involves the flow of fluid only. Therefore, the materials in this simulation was just the atmospheric air. At 25 ℃ and 1 atm pressure, the density of the air is 1.184 kg/m^3 and the dynamic viscosity is 1.849×10^{-5} kg/(m·s) (EngineerEdge, 2020). The setting for materials is shown in Figure 3.18.

Figure 3.18: Materials Selection

3.5.6 Cell Zone Conditions

There were two zones created in the simulation, which were the filter and the fluid. Both zones were set as fluid type. However, the filter was set as porous zone, and the porous formulation was set at physical velocity. By using physical velocity throughout the flow, the porosity is considered in the differential terms of the transport equations to obtain accurate results when velocity gradients are important. Figure 3.19 shows the configurations of cell zone conditions.

Figure 3.19: Configurations of Cell Zone Conditions

3.5.7   Determining the Porous Coefficients

Before proceeding with the simulation of porous media model on pleated design, a set of simulations was done based on the flat sheet model to obtain the porosity. By referring to the experimental data provided by the manufacturer in the form of pressure drop against velocity through the filter media of thickness Δn, it can be extrapolated to obtain the coefficients for the porous component. Table 3.2 shows the experimental data of Arioso media provided by Lydall Performance Material. Figure 3.20 shows the xy curve of pressure drop against velocity. Then, the trendline of the curve was obtained and formed the Equation 3.6.

Table 3.2: Experimental Data of Arioso Media (Lydall, 2016)

Velocity (m/s)	Pressure Drop (Pa)
0.01	3.10862
0.02	13.2281
0.03	23.1497
0.04	33.2692
0.05	43.1908
0.05137	44.5797
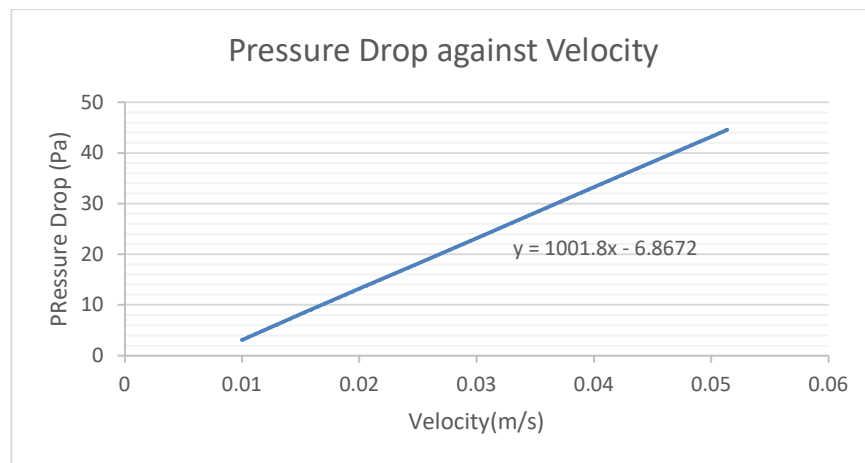
Figure 3.20: Graph of Pressure Drop Against Velocity on Arioso Media

$$\Delta p = 1001.8V - 6.8672 \qquad (3.6)$$

where

$\Delta p =$ pressure drop, Pa

$V =$ velocity, m/s

Hence, by comparing Equation 3.6 to Equation 3.3, the following coefficients can be obtained in Equation 3.7.

$$1001.8 = \frac{\mu}{\alpha} \Delta n$$

(3.7)

With $\mu = 1.849 \times 10^{-5}$ kg/(m $\cdot$ s) and $\Delta n = 0.00034$ m, the viscous inertial resistance factor, $\frac{1}{\alpha} = 1.59355 \times 10^{11}$. Then, the viscous inertial resistance factor was inserted into the porous zone configurations as shown in Figure 3.21. The inertial resistance was set as zero as stated in Chapter 3.3.1. In order to check the validity of the simulation, the simulated results will be compared with the experimental data in Table 3.2 and discussed in Chapter 4.
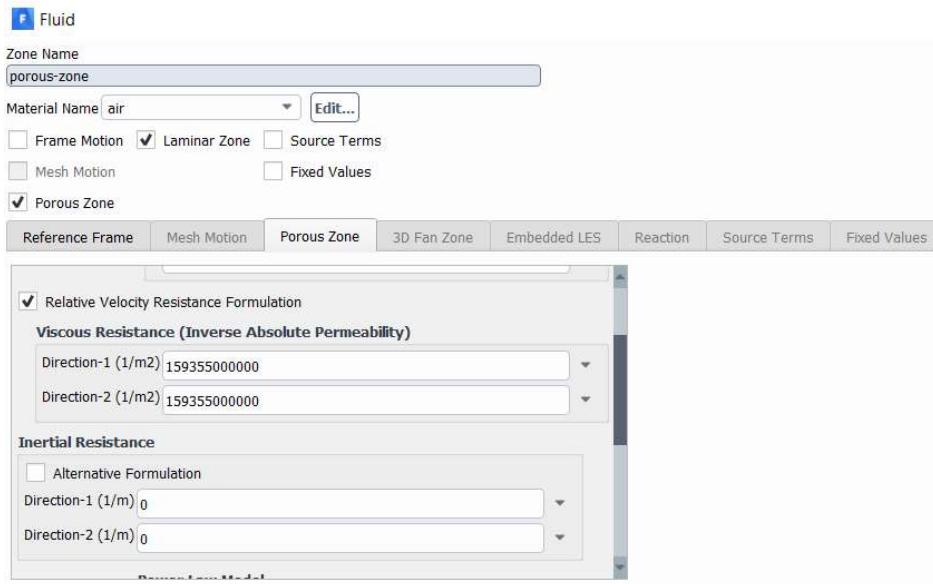
Figure 3.21: Configurations of Porous Zone

3.5.8 Model Boundary Conditions

For flat sheet air filter media, the inlet velocity was determined based on the product sheet of "Arioso" filter media as provided in Figure 3.6, which is from 0.01 m/s to 0.05137 m/s (Lydall, 2016). For pleated air filter media, the input velocity was determined based on the rated airflow volume through the HEPA filter in the property sheet of "Absolute Filter THINFIL Minipleat" (Cambridge

Filter Corporation, 2006). Two different rated airflow volume were suggested at 10 m^3/min and 30 m^3/min. By considering the width and height of the air filter were 0.61 m as stated in Chapter 3.4.1, the inlet velocity of airflow was found to be 0.448 m/s and 1.344 m/s. Hence, the input range of velocity of air flow through pleated air filter is from 0.448 m/s to 1.344 m/s. For each set of simulation, the inlet velocity profile is uniform. Both top and bottom of the numerical domain were set as symmetry boundary condition. The flow was assumed to be a continuative flow until the end of downstream. Hence, the velocity profile at the outlet was uniform, provided that the length between the inlet and the outlet was ensured to be long enough. The gauge pressure was set to be zero as a reference for the upstream. For the wall of the filter and the fluid, stationary wall with no slip condition was set in simulation.

3.5.9   Solution

This subchapter involves the settings which were set to compute the solution for the fluid flow based on the configurations in the Chapter 3.5. The settings of the solution include the methods, residual, initialization and calculations.

The solution methods applied in the simulation is SIMPLE scheme for pressure-velocity coupling as shown in Figure 3.22. SIMPLE has been a preferred method for the solving the computations which involves pressure and velocities (Wiegmann et al., 2009).
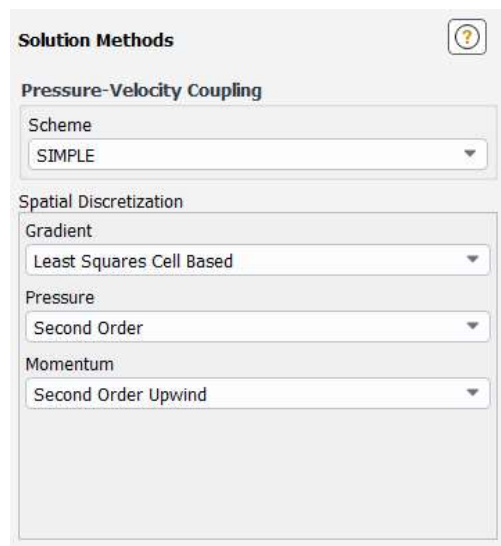
Figure 3.22: Solution Methods

3.5.10 Residual Monitors

The iterations to store was set at 1000 as shown in Figure 3.23. The convergence criterion was absolute. The residual is compared to the criterion at 0.0001 in simulation. If the residual is less than 0.0001, the equation is converged.
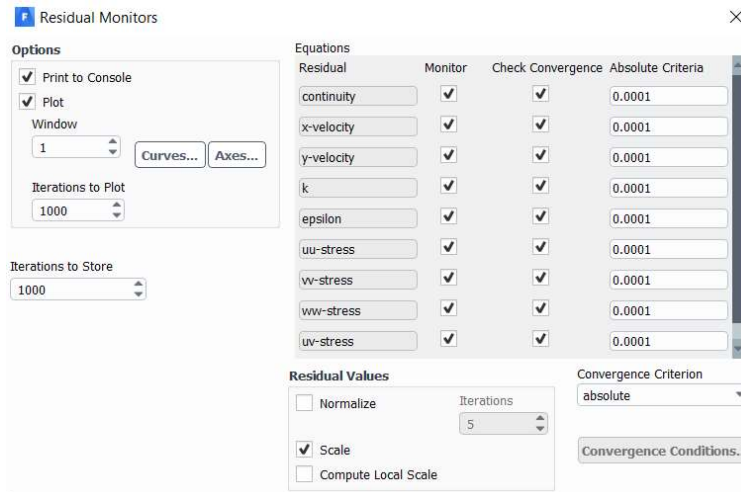
Figure 3.23: Residual Monitors for Reynolds Stress Model (RSM)

3.5.11 Solution Initialization

Standard Initialization was used to initialize the porous media simulations because this type will take in the porous media properties. Figure 3.24 shows that the initialization was computed from inlet.
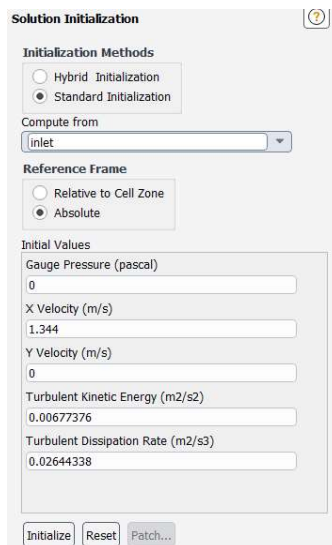
Figure 3.24: Solution Initialization

3.5.12   Run Calculation

In calculation, the number of iterations were set at 1000 as shown in Figure 3.25.
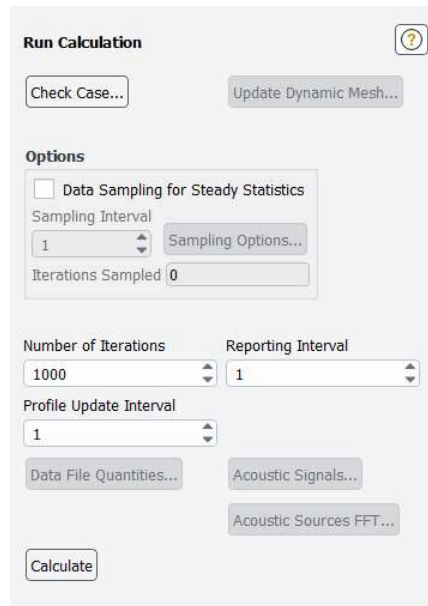
Figure 3.25: Calculation Activities

3.5.13   Results

Figure 3.26 shows that *XY* plane was created on the surface of the pleat body. On the plane, pressure contour was created to present the computational results of the fluid flow through the filter media. Velocity vector and streamlines plots were also created to observe the velocity of the fluid throughout the simulation. Function calculator will be used to determine the value of the results in the simulation.
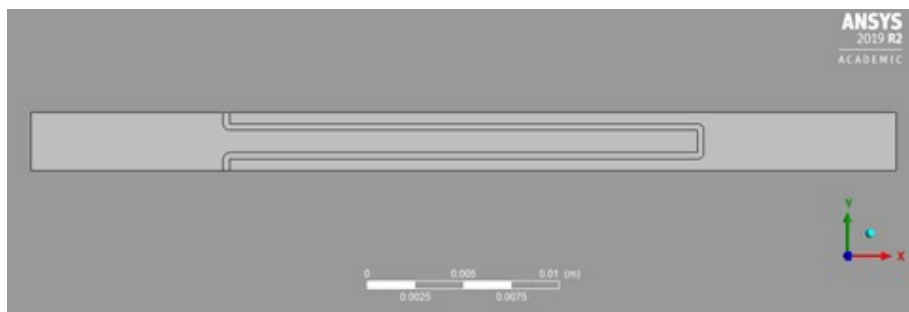
Figure 3.26: *XY* Plane

3.6   Concluding Remark of Methodology

There were two phases involved in the research project: design phase and simulation phase. Firstly, the design is initiated by the external dimension of "Absolute Filter THINFIL Minipleat" from Cambridge Filter Corporation. Pleats with V-shaped and rectangular shape were considered in the design of filter media. A range of 1.5 mm to 6 mm of pleat distances were suggested based on the previous studies. Besides, two different pleat height at 25 mm and 35 mm were involved in the study as well. The overall design of pleated air filter models with different geometrical parameters were generated by using Solidworks.

Simulation phase was started by creating a single pleat in 2D geometry for each type of design by Ansys Fluent due to the symmetry in pleat geometry. Meshing was done on the computational domain with MultiZone method and face sizing. The top and bottom boundary conditions were set as symmetry. At inlet, airflow velocity was suggested from the range of 0.448 m/s to 1.344 m/s. The exit was set as pressure outlet. Throughout the study, "Arioso M70" series from Lydall was selected to be the filter media and assigned as the laminar porous zone. The porous coefficient was obtained according to Darcy's Law. An *XY* plane was created to plot the pressure contour, velocity streamline, and velocity vectors for every set of simulations.

To ensure the accuracy and validity of the results are guaranteed, model validation and mesh validation were performed. Prior to the study on pleating, simulation was performed on a flat sheet porous media to check validity against the experimental data. Grid independence test had been performed to select the preferable mesh size.

CHAPTER 4

RESULTS AND DISCUSSION

4.1   Introduction

The current chapter includes the results and discussion of the study. The simulation results were obtained from the Ansys Fluent software to investigate the pressure drop on the air filtration media. The discussion of the investigation on the pressure drop were made based on the influence of the configurations of the filtration media in terms of pleat shape, pleat distance, and pleat height.

4.2   Validation in Simulation

This sub-chapter presents the results of validation in the simulations generated by Ansys Fluent. The accuracy of the results in model validation and mesh size validation showed that the validity of simulation results was guaranteed.

4.2.1   Model Validation for Flat Sheet Media

Model validation had been performed in the simulation of flat sheet media based on the experimental data provided by the manufacturer as stated in Chapter 3.3. Figure 4.1 shows the graph of comparison between the experimental data and the results of simulation, which were obtained from the simulation of air flow through the flat porous media under grid size of 0.05 mm. It can be determined that the simulation results were in strong agreement with the experimental data. The trendlines of both graphs show positive gradient along the lines. The pressure drop on the flat sheet media increases linearly with the inlet velocity of air flow. As the inlet velocity of the fluid raise from 0.01 m/s to 0.05137 m/s, the pressure drop in the experimental data increased from 3.109 Pa to 44.580 Pa. Whereas, the pressure drop in the results of simulation increased from 3.169 Pa to 44.606 Pa. The greatest percentage difference between the experimental data and the simulation results was determined at the first point of the graphs when the inlet velocity was at 0.01 m/s, which is approximately 1.92 %. It shows that input of porous properties for the model of filter media as stated in Chapter 3.5.7 is accurate. Therefore, the validation of the model created in the simulation throughout this study is guaranteed by the accuracy of the simulated results.
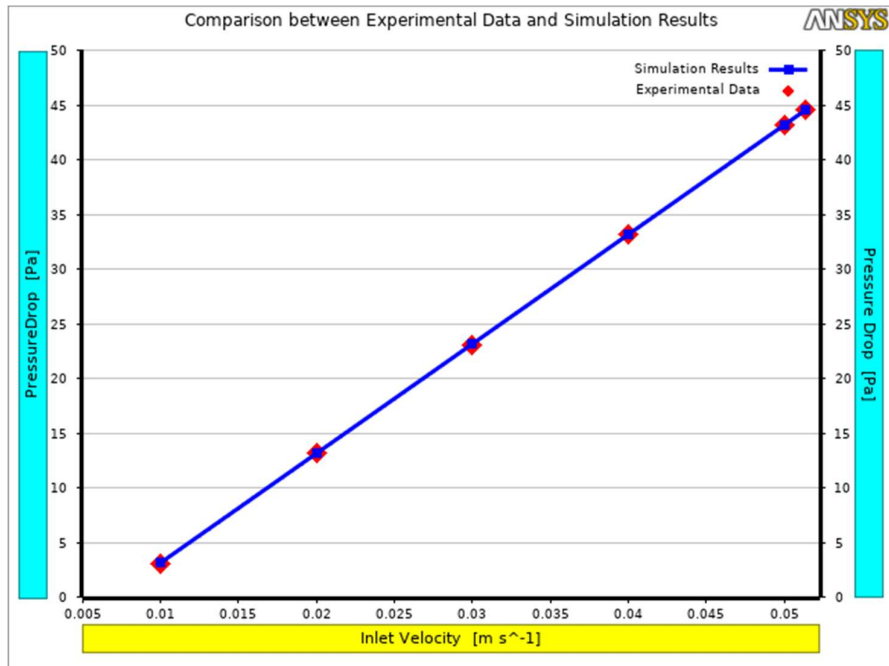
Figure 4.1: Graph of Comparison between Experimental Data and Simulation Results

4.2.2 Mesh Size Validation

Figure 4.2 shows the grid independence test of result based on eight grid systems.
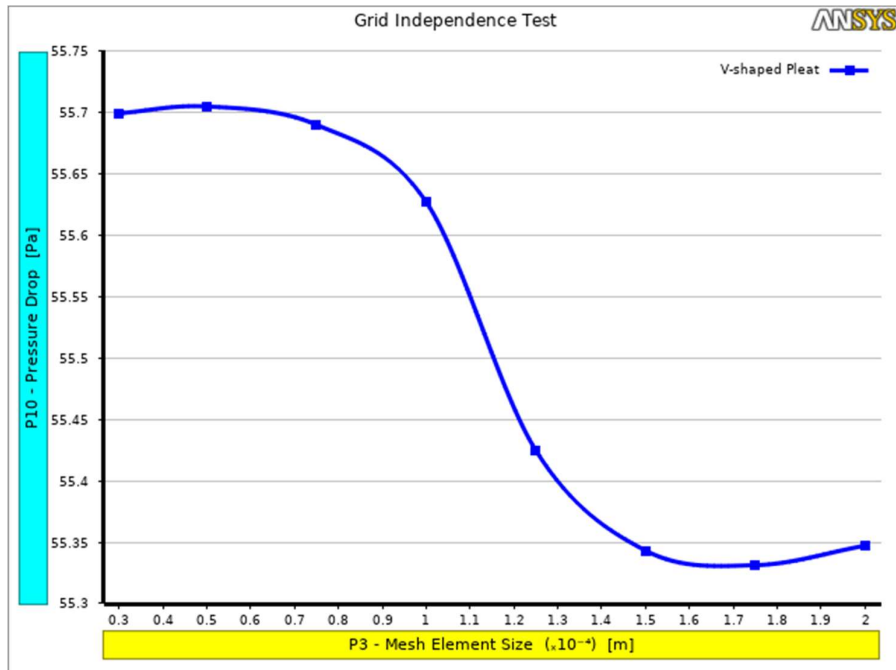
Figure 4.2: Graph of Grid Independence Test

The generated model was meshed with eight sets of grid size by varying the mesh element size from 0.03 mm to 0.2 mm as mentioned in Chapter 3.5.2. Based on Figure 4.2, the pressure drop were varied from 55.35 Pa to 55.70 Pa for every type of meshes in the case of the configuration of media pack was pleated in V-shaped at 6 mm pleat distance and 25 mm pleat height with inlet velocity of 0.448 m/s. It was noticed that the pressure drop had not changed much when the mesh size was in the range of 0.03 mm to 0.075 mm. Therefore, mesh element size at 0.05 mm was selected in between to achieve the accuracy and validity of results, while avoiding excessive time for each set of simulation.

4.3 Effect of Pleating on Flat Sheet Media

Figure 4.3 shows the comparison of simulation results regarding pressure drop from the simulation of the fluid flow through flat sheet media and pleated media. The properties of the fluid and porous media were constant in terms of density, thickness and permeability. The pleated media was V-shaped at 6 mm pleat distance and 25 mm pleat height. Based on Figure 4.3, it can be observed that the pressure drop on both types of filtration media increases linearly with the inlet velocity of air from 0.01 m/s to 0.05137 m/s. The pressure drop for flat sheet media increased linearly from 3.169 Pa to 44.606 Pa. Whereas, the pressure drop for pleated media increased linearly from 1.244 Pa to 6.403 Pa.
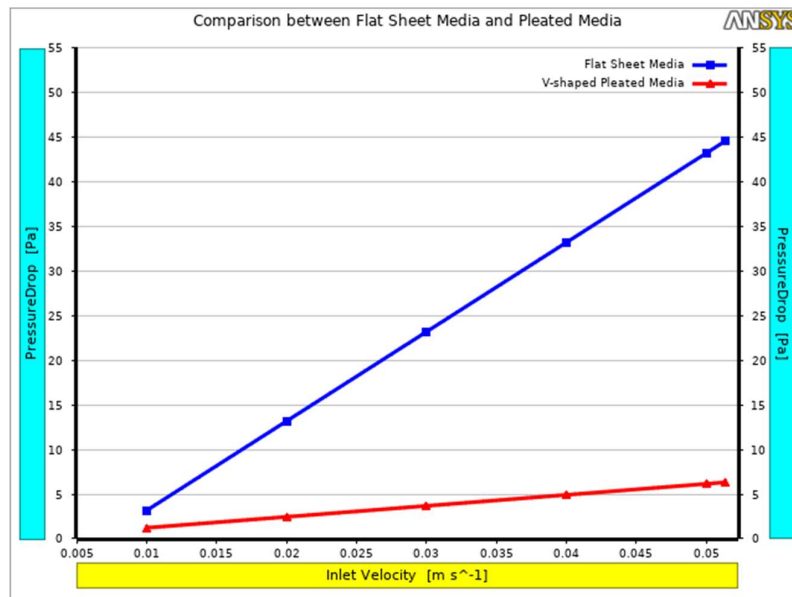
Figure 4.3: Graph of Comparison between Flat Media and Pleated Media

The fact that pleated media produced lower pressure drop can be explained by the fact that large filtration area can reduce the filtration velocity through the media. The explanation is in good agreement with the study conducted by Al-Attar et al. (2011). Figure 4.4 and Figure 4.5 show the velocity vector plots of simulation at 0.02 m/s on the flat sheet media and pleated media respectively. By looking into Figure 4.4 and Figure 4.5, it was clear that the surface area of the V-shaped pleated media was larger than the surface area of flat sheet media. The filtration velocity at flat sheet media remained at 0.02 m/s, but the velocity at the surface of pleated filtration media had been reduced to around 0.015 m/s. It is due to the fact that larger filtration area was allowed for the diffusion of particles. According to Darcy's law as stated in Chapter 3.3.1, the pressure drop decreases linearly with the decrease in filtration velocity. This implies that low pressure drop can be obtained by maximizing the filtration area.
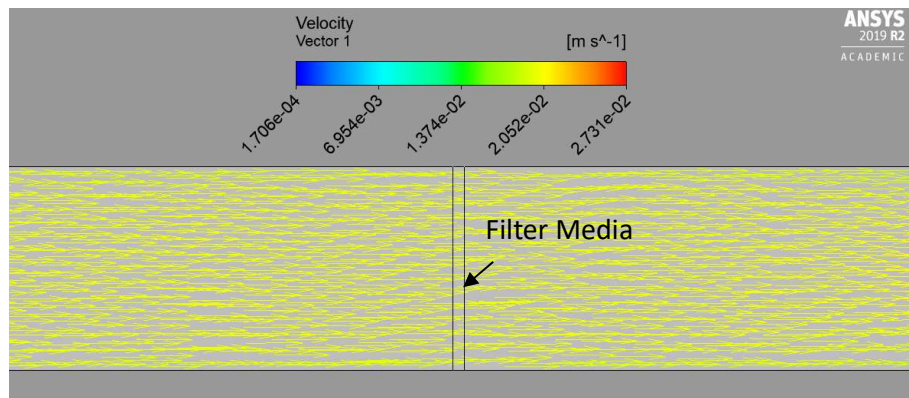
Figure 4.4: Velocity Vector Plot of Simulation on Flat Sheet Media
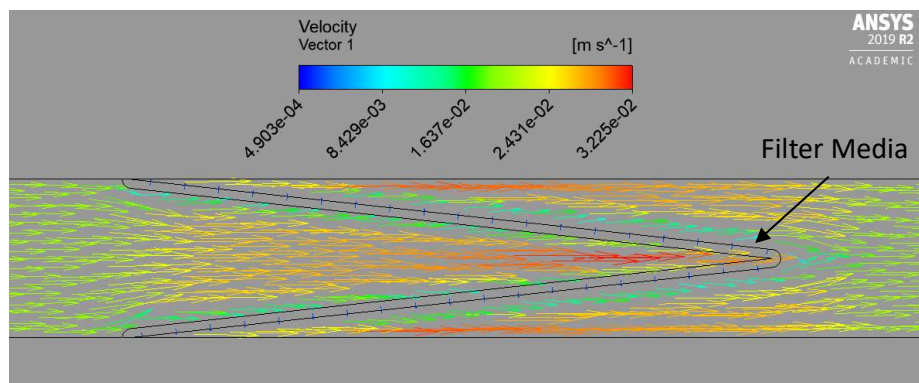
Figure 4.5: Velocity Vector Plot of Simulation on V-shaped Pleated Media

Figure 4.6 and Figure 4.7 shows the pressure contour plot of simulation for air velocity at 0.02 m/s on flat sheet media and pleated media respectively. It can be observed that when the air was flowing at the direction to the right, the pressure drop happened at the interface of porous media. For flat sheet media, the pressure drop was evenly on the media. Whereas for the V-shaped pleat, the pressure drop on pleated media was found larger at the front-end tip at entrance, while lower at the back-end tip at the exit. It can be explained by the fact that the ratio of surface area between both sides at each tip was huge. When the air was flowing through the front end of pleat, the air flow was converged into the smaller space. More impacts of collisions between particles were happened, thus producing greater pressure drop. When the air was flowing out from back end, there were lesser air particles in the stream, thus producing lower pressure drop.
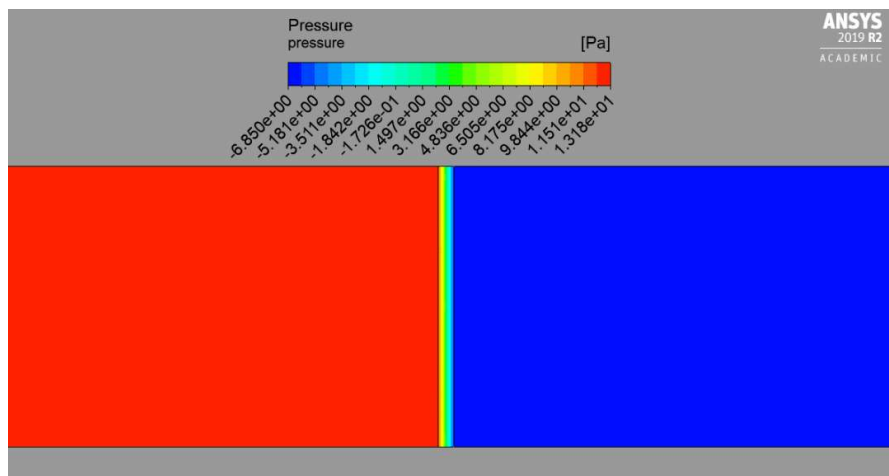
Figure 4.6: Pressure Contour Plot of Simulation on Flat Sheet Media
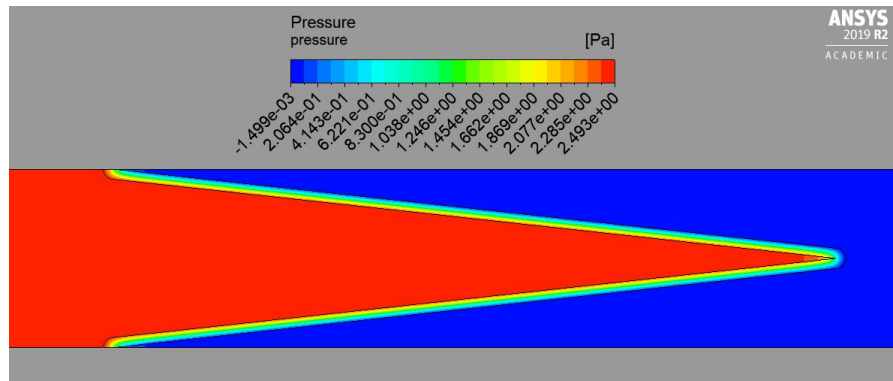
Figure 4.7: Pressure Contour Plot of Simulation on V-shaped Pleated Media

4.4   Configurations of Media Pack by Pleat Shape, Pleat Distance, and Pleat Height

This sub-chapter discusses the optimum characteristics of the pleat geometry on media pack configuration in terms of pleat shape, pleat distance, and pleat height.

4.4.1   Effects of Pleat Shape on Pressure Drop

Figure 4.8 shows the comparison of results from the simulation of air flow through V-shaped pleated media and rectangular pleated media as stated in Chapter 3.5. Both porous media had 3 mm pleat distance and 25 mm pleat height. The results indicate that increased inlet velocity resulted in rise in pressure drop, which can be explained by Darcy's law. However, it was clearly noticed that the rise in pressure drop on rectangular pleat was larger than the rise in pressure drop on V-shaped pleat. When the inlet velocity of air was around 0.88 m/s, the pressure drop on both types of pleated media were approximately similar. For air flow with inlet velocity in the range between 0.448 m/s and 0.88 m/s, the pressure drop on V-shaped pleat was greater than on rectangular pleat. However, the results were found in opposite when the velocity was in the range between 0.88 m/s and 1.344 m/s. It can be explained based on Figure 4.9 and Figure 4.10.
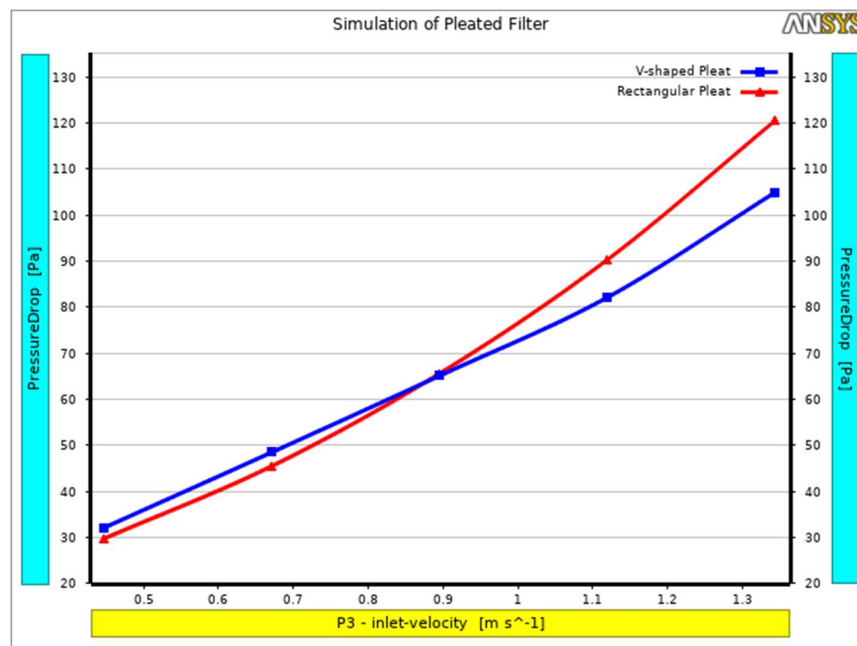
Figure 4.8: Graph of Comparison between Simulation for V-shaped Pleat and Rectangular Pleat with Various Inlet Velocity

Figure 4.9 and Figure 4.10 shows the pressure contour plot of simulation for air velocity at 0.448 m/s on rectangular pleat and V-shaped pleat respectively. The pressure drop happened upon the fluid approaching the pleat channel of both type of media, followed by gradually drop at the interface of porous media. By looking into the Figure 4.9 and Figure 4.10, it can be determined that the rectangular pleated media has larger surface area than V-shaped pleated media. A plausible explanation for the rectangular pleat to have lower pressure drop at low filtration velocity is the effect of surface area of as discussed in Chapter 4.3. The larger filtration area in the rectangular pleat channel had reduced the flow velocity of the fluid at the surface of media and thus reduced the pressure drop.
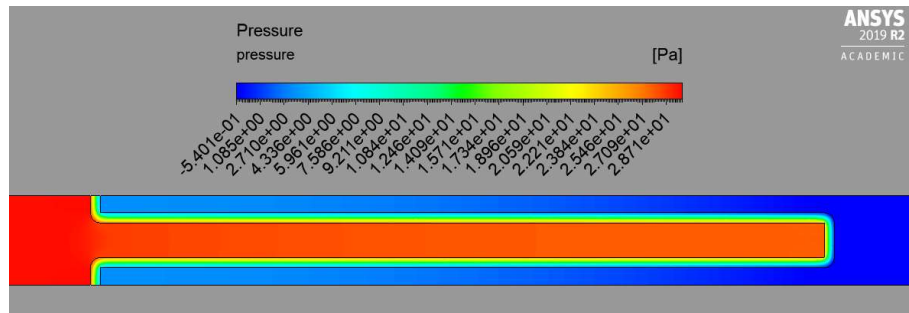
Figure 4.9: Pressure Contour Plot for Rectangular Pleat with inlet velocity of air at 0.448 m/s
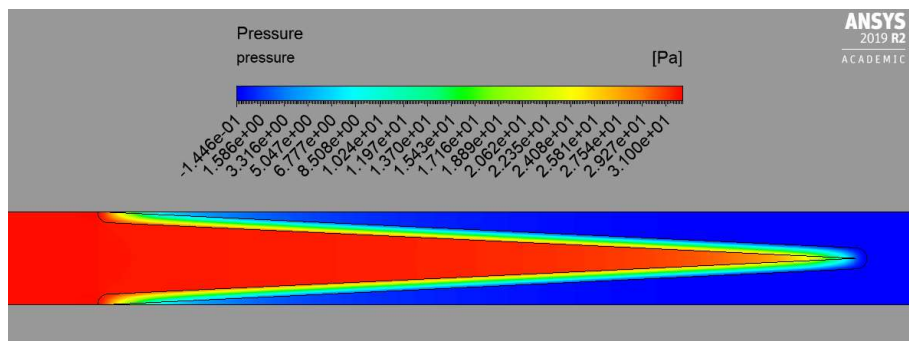
Figure 4.10: Pressure Contour Plot for V-shaped Pleat with inlet velocity of air at 0.448 m/s

However, as inlet velocity of air was increasing, the difference between pressure drop for both types of media became smaller as shown in Figure 4.8, and eventually the pressure drop on rectangular pleat became larger than on the V-shaped pleat. It can be explained by looking into Figure 4.11 and Figure 4.12.

Figure 4.11 and Figure 4.12 show the streamline plot with inlet velocity of air at 0.448 m/s on the rectangular pleated media and V-shaped pleated media. It can be observed that both types of simulation possess the same characteristics of fluid flow through the filtration media. When the fluid flow was approaching the filter media, flow contraction was in the upstream of the pleated filter region. Most of the fluid squeezed into the upstream pleat channel while the rest had directly passed through the front end of the filter media. The sudden contraction had caused the air to accelerate for a short distance in rectangular pleat, but longer distance in V-shaped pleat due to the channel was getting narrower until the back end. Fluid flow direction at the porous media was normal to the surface. Upon exiting the media into the downstream pleat channel, air started to accelerate due to the mass injection from the porous media. There was only little flow that passed through the back end of the pleated filters. Upon leaving the filter region, flow expansion was observed, and the flow profile in both types of media had slowly recovered to the uniform condition in different distance.
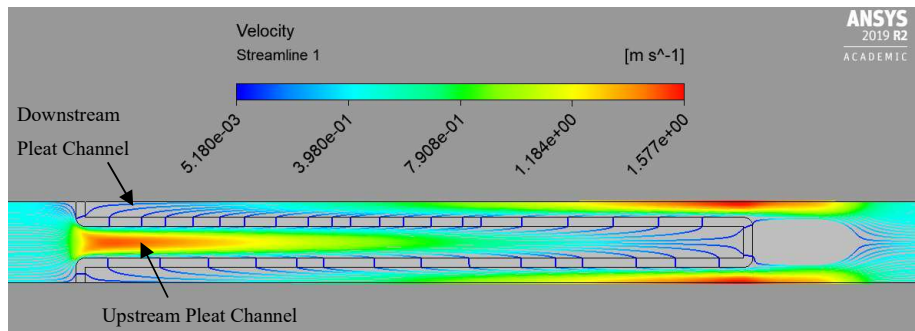
Figure 4.11: Streamline Plot on Rectangular Pleated Media with inlet velocity of air at 0.448 m/s
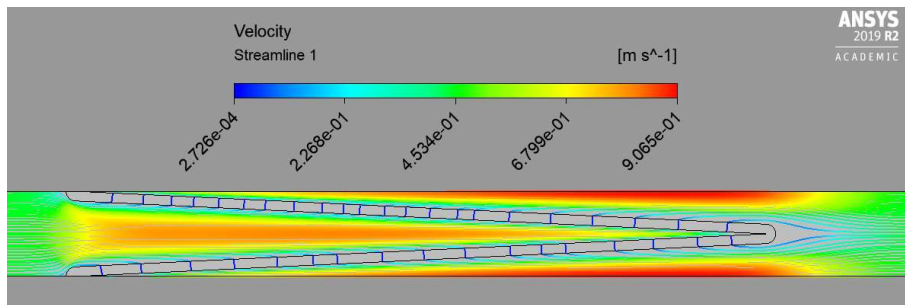
Figure 4.12: Streamline Plot on V-shaped Pleated Media with inlet velocity of air at 0.448 m/s

It was mentioned that the results shown in Figure 4.8 have indicated that the pressure drop on rectangular pleat had become larger than on V-shaped pleat. It is due to the fact that the effect of large surface area had become insignificant with the increase in velocity of air flow. This explanation is in agreement with the general finding of Maddineni, Das and Damodaran (2019), whereby the inertial effect and viscous drag of the fluid at narrow pleat channel had become more dominant than the effect of large surface area. The higher the flow velocity, the greater the inertia it has. Additional pressure drop was raised from the inertia for the streamlines to avoid taking the shortest path through the high resistance media. Figure 4.13 shows the pressure contour plot for air velocity at 1.344 m/s on rectangular pleat.
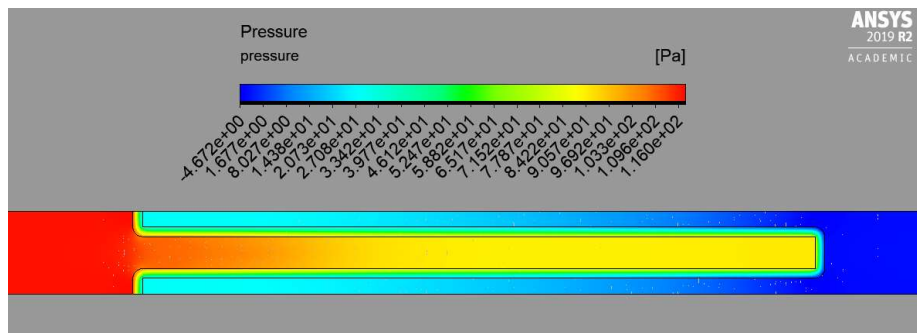
Figure 4.13: Pressure Contour Plot for Rectangular Pleat with inlet velocity of air at 1.344 m/s

It can be clearly noticed that the pleat space at the upstream of the rectangular pleat was smaller than at the V-shaped, hence inertial effect was stronger for flow contraction and expansion at high flow velocity in the rectangular pleat. Besides, when the flow was suddenly contracted into the upstream pleat channel, the velocity gradient increased with the inlet velocity. The greater the velocity gradient, the greater the laminar and turbulent viscous drag on the flow, hence rising the pressure drop. Due to the narrower pleat space at the rectangular pleat channel, the contraction and expansion of fluid were more significant, so the velocity gradient was stronger. The higher the velocity of the flow, the greater the viscous drag effect, thus increasing the pressure drop. Figure 4.14 shows the pressure contour plot for air velocity at 1.344 m/s on the V-shaped pleat.
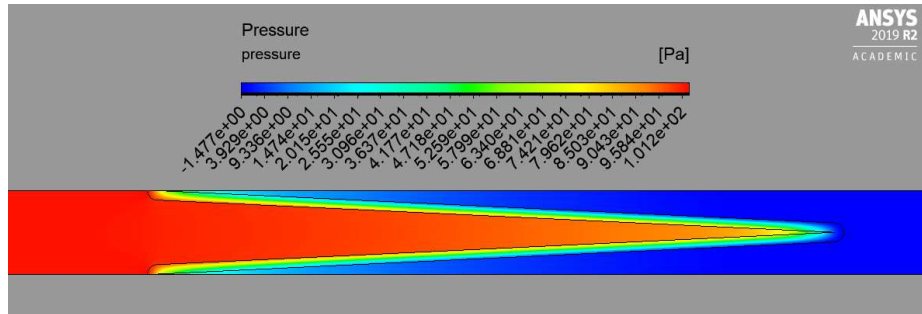
Figure 4.14: Pressure Contour Plot for V-shaped Pleat with inlet velocity of air at 1.344 m/s

By comparing the results shown in Figure 4.13 and Figure 4.14, it was observed that a strong pressure distribution was built up at the upstream of rectangular pleat channel. Whereas the pressure drop happened almost evenly on the surface of V-shaped pleat at lower values. This provides clear evidence that the effects of inertial and viscous drag were greater on rectangular pleat at high inlet velocity of air flow.

Therefore, this implies that the overall pressure drop on the pleated filter is affected by two factors. One contributing factor is the result from the filtration flow through the porous medium according to Darcy's law. The increase in total filtration area could reduce the filtration velocity, thus reducing pressure drop. The second factor is due to the result from the effects of inertia and viscous drag within the pleat channels. The greater the contraction and expansion of the flow at pleat channels, the greater the inertial effect as well as the velocity gradient. When the filtration velocity increases, the viscous drag becomes stronger, thus increasing the pressure drop. These factors are in strong agreement with the finding of Chen, Pui and Liu (1995). Therefore, when the fluid particles are highly inertial, V-shaped pleat geometry is preferred over the rectangular pleats due to less pressure drop. On the other hand, rectangular pleat geometry is better when the inlet velocity is low.

4.4.2   Effects of Pleat Distance on Pressure Drop

Figure 4.15 shows the comparison of results in terms of pressure drop on both V-shaped pleat and rectangular pleat with a range of pleat distance form 1.5 mm to 6 mm. The inlet velocity was fixed at 0.448 m/s and pleat height was 25 mm.
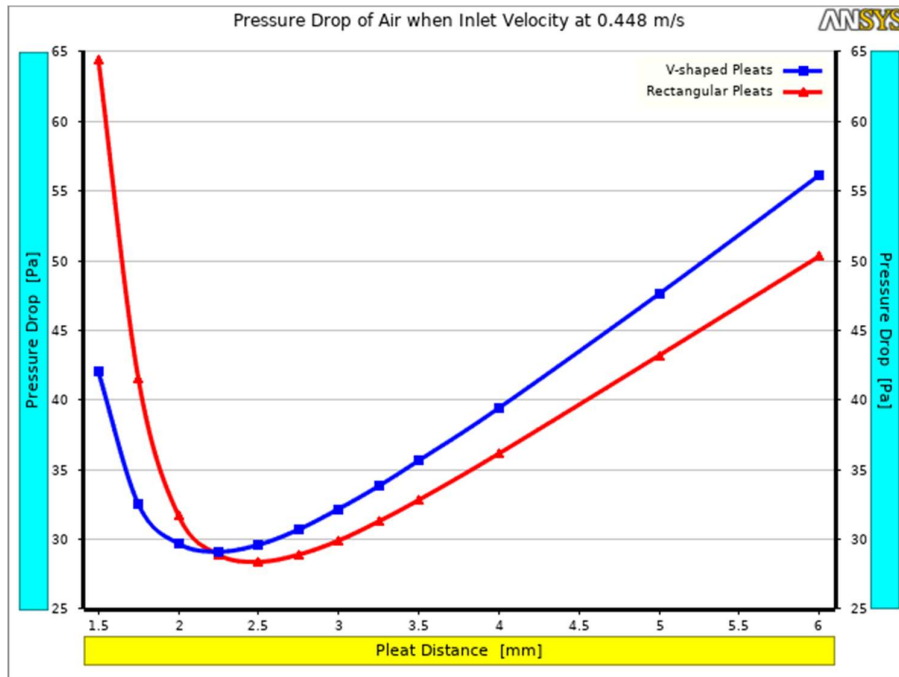
Figure 4.15: Graph of Comparison between Simulation for V-shaped Pleat and Rectangular Pleat with Various Pleat Distance at 0.448 m/s

Based on Figure 4.15, the results indicate that the both types of pleated media have the similar trendlines when the pleat distance changed from 1.5 mm to 6 mm. The typical U-shaped curve is similar to the results obtained by Chen, Pui and Liu (1995). When the pleat distance changed from 1.5 mm to 6 mm with constant pleat height at 25 mm, the pressure drop reduced with higher pleat distance until 2.25 mm on V-shaped pleat and increased thereafter. Similarly, the pressure drop on rectangular shape decreased with increased pleat distance until 2.5 mm followed by increase. However, the pressure drop on V-shaped pleat was greater than on rectangular pleat at their optimum points. The corresponding pressure drop values were 29.118 Pa and 28.394 Pa for 2.25 mm of V-shaped pleat distance and 2.5 mm of rectangular pleat distance respectively. Besides, the pressure drop on rectangular pleat was significantly greater than on V-shaped pleat at low pleat distances, while smaller at high pleat distances.

The fact that the U-shaped curve was obtained in the range of pleat distance can be explained by referring to the discussion made in Chapter 4.4.1. As mentioned earlier, the overall pressure drop on a pleated filter are contributed by the filtration area of filter medium and the effects of drag at pleat channel.

The optimal point, which is the optimum pleat distance, was obtained when the trade-off between the two factors had led to the lowest pressure drop on media. In general, the number of pleats on a filter media increases when the pleat distance reduces. Figure 4.16 shows the number of V-shaped pleats in 30 mm width for pleat distances at 6 mm and 3 mm. The greater the number of pleats, the larger the available area for filtration. The large filtration area reduced the filtration velocity, thus reducing pressure drop according to Darcy's law. Hence, the pressure drop decreased with the decreased pleat distance until optimal point.
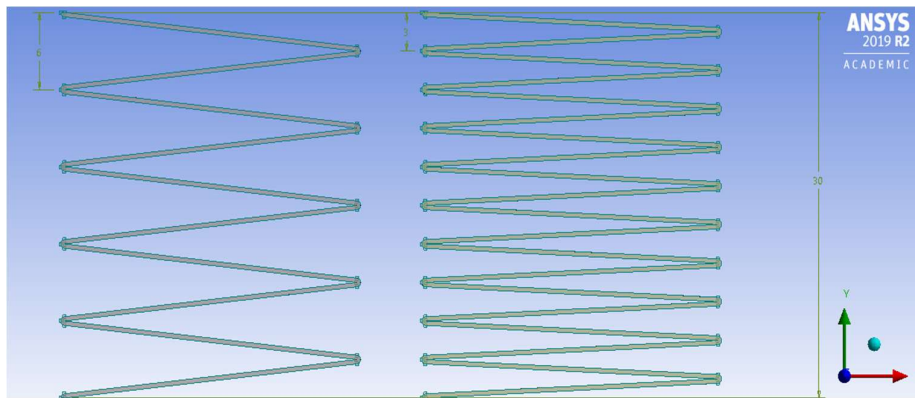
Figure 4.16: Number of V-shaped Pleats in 30 mm Width Media

Next, the fact that the increase in pressure drop had took place when the pleat distance reduced to below optimal point was due to the fact that the pleat space had become too narrow, which caused the inertial effects to get dominant even though the filtration area was large. Figure 4.17 and Figure 4.18 show the streamline plot with inlet velocity of air at 0.448 m/s on the rectangular pleated media and V-shaped pleated media respectively at 1.5 mm pleat distance.
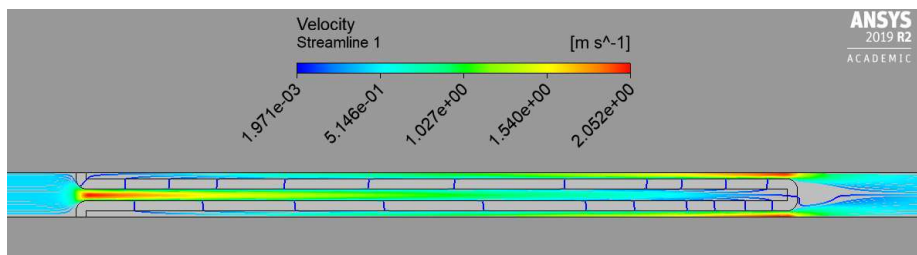
Figure 4.17: Streamline Plot on Rectangular Pleated Media with inlet velocity of air at 0.448 m/s and 1.5 mm Pleat Distance
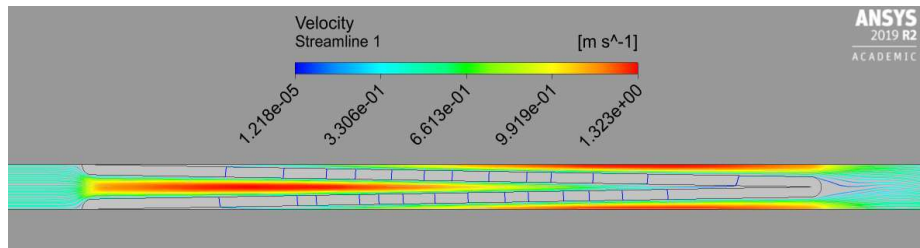
Figure 4.18: Streamline Plot on V-shaped Pleated Media with inlet velocity of air at 0.448 m/s and 1.5 mm Pleat Distance

By comparing Figure 4.11 to Figure 4.17 and Figure 4.12 to Figure 4.18, it can be observed that the flow contraction at the entrance of pleat channel was more significant at 1.5 mm pleat distance for both type of pleat shape, thus contributing to stronger inertial effect. The narrow space at pleat channel had forced the air flow to contract and expand with strong acceleration. Figure 4.19 shows the maximum velocity of air flow in the pleat channels with inlet velocity at 0.448 m/s. The velocity was increased when the pleat distance decreased due to the stronger acceleration in contraction and expansion at the pleat channels. This led to greater viscous drag due to higher velocity gradient, thus increasing pressure drop when pleat distance was reduced, especially on rectangular pleat.
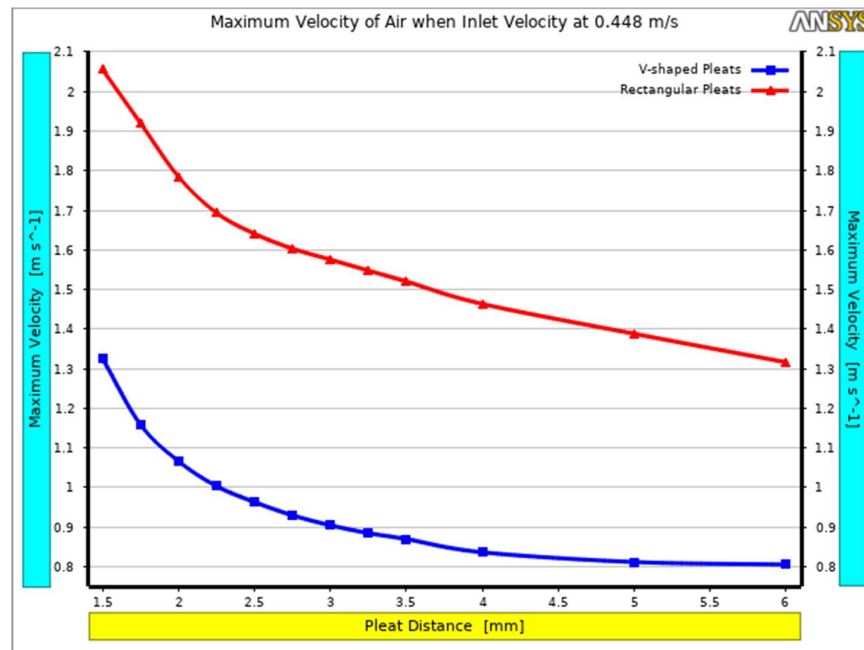
Figure 4.19: Maximum Velocity of Air Flow in Pleat Channel with Inlet Velocity at 0.448 m/s

The effect of over-pleating on filter media which caused an increase in the viscous drag in the pleat channel is also known as pleat crowding (Al-Attar et al., 2011). Figure 4.20 shows the pressure drop on both types of pleated media with similar range of pleat distance, but inlet velocity was changed to 1.344 m/s. The optimal point for V-shaped pleat was 113 Pa at 2.75 mm pleat distance, while for rectangular pleat was 130.25 Pa at 3.25 mm pleat distance. The optimal point for both types of pleated media was shifted to the right. Also, the minimum pressure drop for V-shaped pleat had become lower than for the rectangular pleat. The results indicate that the effect of pleat crowding was more significant in this case of higher inlet velocity, especially in the rectangular pleat due to narrower pleat channel. The effect of inertial and viscous drag was more dominant than the effect of filtration area for the trade-off at high inlet velocity.
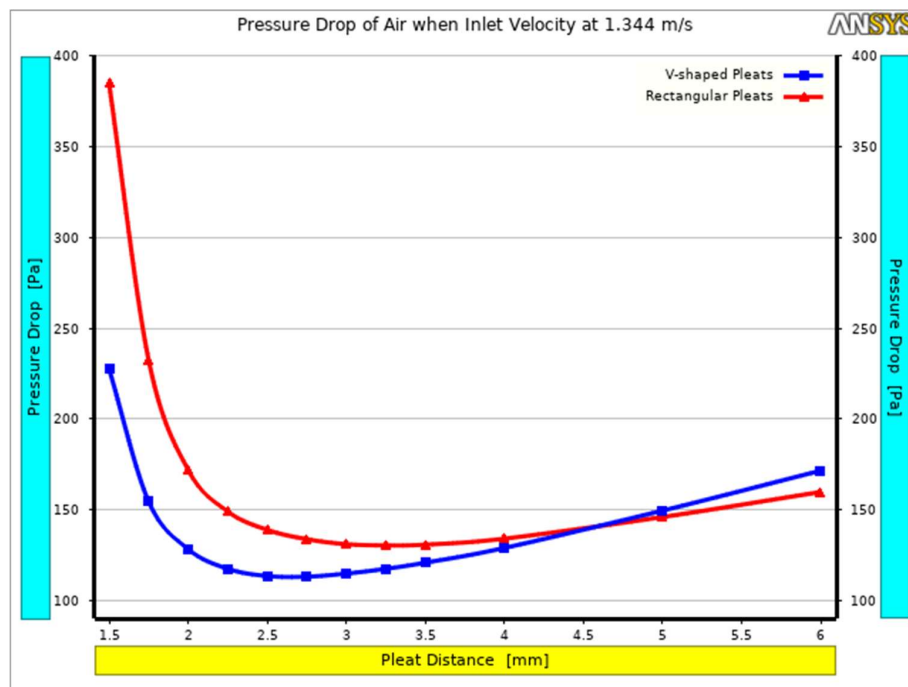
Figure 4.20: Graph of Comparison between Simulation for V-shaped Pleat and Rectangular Pleat with Various Pleat Distance at 1.344 m/s

Hence, this implies that the pleat distance on a filter media could affect the overall pressure drop by the effect of flow through medium and pleat channel. Minimum pressure drop can be obtained at optimal pleat distance by getting a trade-off between filtration area and the air drag on both types of pleated media.

4.4.3 Effects of Pleat Height on Pressure Drop

Figure 4.21 and Figure 4.22 show the comparison of pressure drop between pleat height at 25 mm and 35 mm with a range of pleat distance from 1.5 mm to 6 mm on the rectangular pleated media and V-shaped pleated media respectively. By looking into both Figure 4.21 and Figure 4.22, it was clearly shown that the pressure drop on the pleated media has been reduced when the pleat height was switched from 25 mm to 35 mm at most of the pleat distance. This is due to the fact that the increase in pleat height will lead to increase in total filtration area, even though the pleat distance is unchanged. The results provide clear evidence that the pressure drop was lower when the filtration area had become larger. The explanation on the effect of increased filtration area on pressure drop can be found from the discussion in Chapter 4.3. However, attention was paid at the pressure loss for pleat distance that smaller than 1.75 mm on rectangular pleat and that smaller than 1.65 mm on V-shaped pleat. It was noticed that pressure loss on pleat height at 35 mm had become larger than on pleat height at 25 mm. One contributing factor is that the effect of viscous drag increased more than the effect of filtration area, hence pressure drop had become larger in this case.
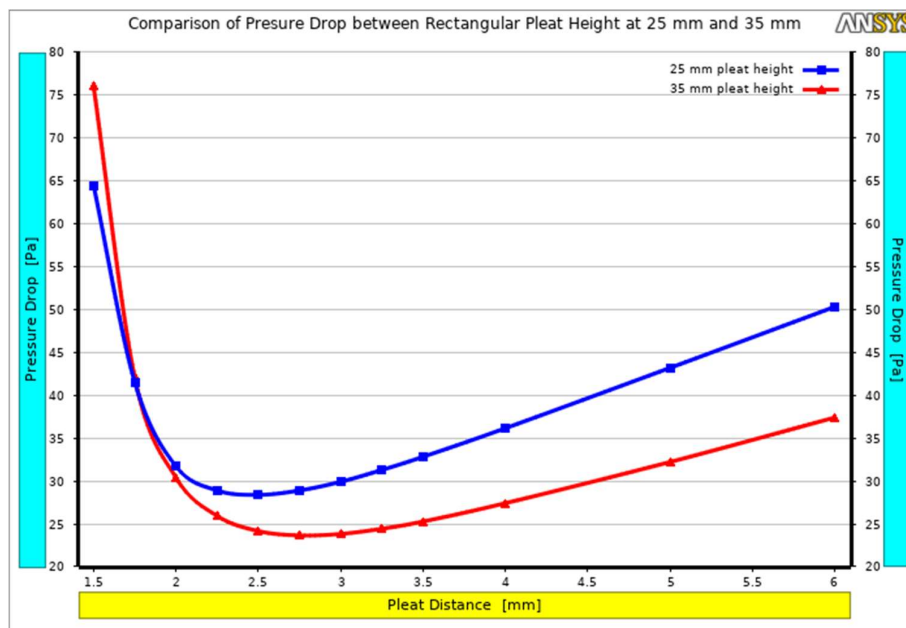
Figure 4.21: Graph of Comparison of Pressure Drop between Rectangular Pleat Height at 25 mm and 35 mm
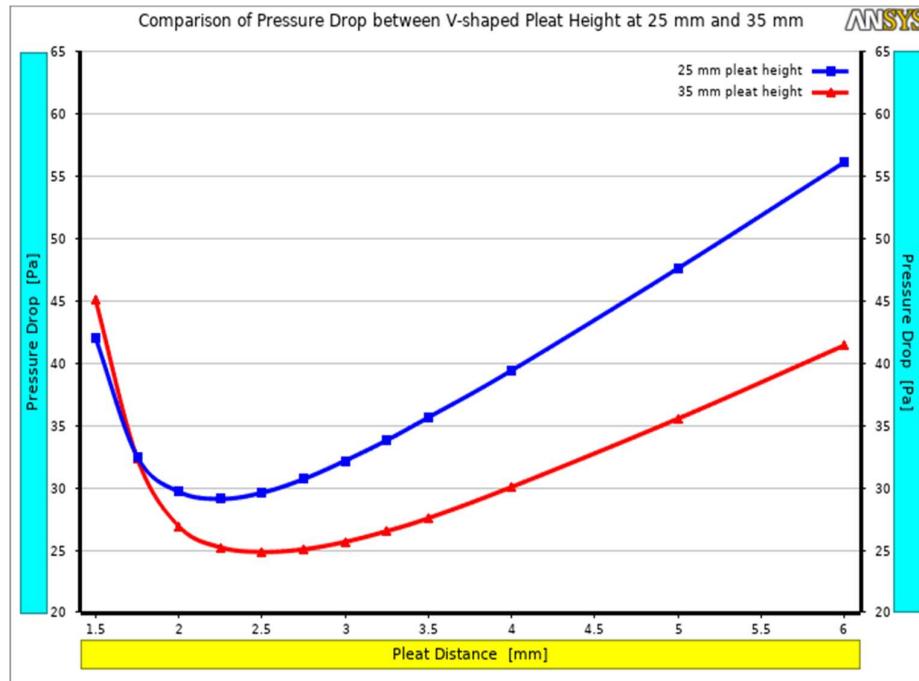
Figure 4.22: Graph of Comparison of Pressure Drop between V-shaped Pleat Height at 25 mm and 35 mm

Furthermore, the results also indicate that the optimal point for minimum pressure loss was shifted to the right when the pleat height was switched from 25 mm to 35 mm. The results appear to confirm the findings of research carried out by Maddineni, Das and Damodaran (2019). For rectangular pleat, the optimal pleat distance was moved from 2.5 mm to 2.75 mm, and the minimum pressure drop was decreased from 28.394 Pa to 23.663 Pa. For V-shaped pleat, the optimal pleat distance was shifted from 2.25 mm to 2.5 mm, and the minimum pressure drop was reduced from 29.118 Pa to 24.866 Pa. It appears that there was an interaction between the pleat distance and the pleat height. So, it is possible to speculate that the optimal point happened at higher pleat distance when pleat height was increased because the rise in viscous drag effect had become dominant at higher pleat distance for the case of large pleat height. Although the optimal pleat distance was increased, the pressure drop was found to be reduced at large pleat height.

Therefore, it implies that minimum pressure drop can be obtained by increasing the pleat height and obtaining the optimal point for pleat depth, with the trade-off between the effects in terms of filtration area and air drag.

4.5   Problems Encountered in the Study

Throughout the entire study, the most critical problem that should be highlighted was the lengthy time taken in both design phase and simulation phase.

4.5.1   Long-running Process of Design Phase and Simulation Phase

In the design phase, Solidworks program was used to generate the 3D model of media pack with various configurations in terms of pleat shape, pleat distance and pleat height. As stated in Chapter 3.4, the external dimensions of the filter media were 610 mm for both height and width, but the distance between the pleats were in the range of 1.5 mm to 6 mm. The ratio between the external dimensions and the pleat distance appeared to be very large, which means that the maximum number of pleats will be 406 pleats per filter. In order to generate large number of pleats, linear pattern in one direction was applied in sketching, followed by creating a boss extrude from the sketch. Lengthy time was spent on this process to generate model for each filter design.

In simulation phase, fine meshes were generated on the computational domain in order to give accurate results, but the time to generate was extended. Although grid independence test had been performed to select the preferable mesh size for simulation, the time to generate the selected mesh size still lengthy. Besides, the process of computation is also long due to large mesh density.

The long-running process took place because the computer used in the current project does not meet the recommended hardware requirements of the software. According to Durksen (2019), the preferable processor (CPU) should have 3 GHz or higher clock speed and random-access memory (RAM) at least 16 GB for Solidworks. For Ansys CFD software, a minimum of 16 GB of RAM is recommended as well (Ozen Engineering Incorporation, 2020). In this project, the computer only has CPU clock speed at 1.8 GHz and 12 GB of RAM, which is lower than the recommendations. Therefore, the lengthy time was spent on these programs because the current hardware is not optimized.

CHAPTER 5

CONCLUSIONS AND RECOMMENDATIONS

5.1   Conclusions

In this study, the influence of media pack configuration for an air filter in terms of pleating shape, pleat distance and pleat height of the media pack was determined. Solidworks program was used to create models of air filter with different design of shape and geometry as shown in Figure 3.12 and Figure 3.13. Ansys Fluent software was used to simulate the flow of the air across the filter media. Results were obtained and discussed based on detailed analysis of the airflow through the filter media. Pressure drop across the filter media was the output parameter to be minimized by optimizing the pleat configurations.

The models of flow through a porous medium in the simulation was validated against the experimental data provided by the manufacturer. The greatest percentage difference between the experimental data and the simulation results was approximately 1.92 %, which shows that the simulated results were in close agreement with the experimental data. In order to achieve the validity in terms of accuracy of result, grid independence test was performed between course and fine meshes ranging from 0.2 mm to 0.03 mm of mesh element size. The preferable mesh element size was selected for each set of simulation.

In conclusion, it was found that the pressure drop on both flat sheet filter media and pleated filter media increased linearly with the airflow velocity, but it is significantly lower on the pleated filter media. The results are in good agreement with the study conducted by Al-Attar et al. (2011). It can be explained by the fact that large filtration area can reduce the filtration velocity. According to Darcy's law, the pressure drop decreases linearly with the decrease in filtration velocity. Another finding from the study is that the overall pressure drop can be influenced by the effects of inertia and viscous drag as well. The greater the contraction and expansion of the flow at pleat channels, the greater the inertial effect as well as the velocity gradient, thus producing greater pressure drop. Therefore, when the fluid particles are highly inertial, V-shaped pleat geometry is preferable due to lower contraction and expansion of airflow. When the fluid particles are low inertial, the rectangular pleat are preferable

because it has larger filtration area. These two factors of overall pressure drop, including filtration area and drag effect, had contributed to the typical U-shaped curve generated in the results, which is in close agreement with the findings of Chen, Pui and Liu (1995). On the curve, the optimum pleat distance was obtained when the trade-off between the two factors had led to the lowest pressure drop on filter media. As the pleat distance increased from the optimal point to the right side, the filtration area decreased because the number of pleats per filter had been reduced, hence increasing pressure drop. As the pleat distance decreased from the optimal point to the left side, the contraction and expansion of airflow increased because the space between the pleats had been reduced, thus increasing pressure drop. Moreover, it was also found that the minimum pressure drop was reduced at large pleat height. The results agrees strongly with the findings of research carried out by Maddineni, Das and Damodaran (2019). It is likely that the large pleat height has large filtration area effect. Therefore, it implies that there is an interaction between the pleat distance and pleat height, the trade-off between them must be achieved for minimum pressure drop.

Lastly, the current work is significant because it provides the techniques of using the software in design and simulation. The findings of the study suggest the optimal geometry in terms of pleat shape, pleat distance and pleat height.

5.2   Recommendations for future work

The notable limitations of the current work were mentioned in Chapter 4.5. Hence, recommendation for the future work will be discussed in this subchapter.

To further improve the accuracy and efficiency in the future work, it is preferable to improve the performance of computer by upgrading the hardware. Computer with processor (CPU) of 3 GHz of clock speed and 16 GB of random-access memory (RAM) are recommended for the applications of Solidworks and Ansys software, so that the data processing speed can be increased.

REFERENCES

AAF, 2017. *Method of Testing General Ventilation Air-Cleaning Devices for Removal Efficiency by Particle Size*. [online] Available at: <www.ashrae.org> [Accessed 21 Apr. 2020].

Air Quality Engineering, 2018. *What Are The Mechanisms Of Filtration*. [online] Available at: <https://www.air-quality-eng.com/air-cleaners/filtration-mechanisms/> [Accessed 21 Apr. 2020].

Al-Attar, I., Wakeman, R., Tarleton, S. and Husain, A., 2010. The effect of pleat count and air velocity on the initial pressure drop and fractional efficiency of hepa filters. *Filtration*, 10(3), pp.202–208.

Al-Attar, I., Wakeman, R., Tarleton, S. and Husain, A., 2011. The effect of face velocity, pleat density and pleat orientation on the most penetrating particle size, pressure drop and fractional efficiency of HEPA filters. *Filtration*, 11(4), pp.248–256.

Allam, S. and Elsaid, A.M., 2020. Parametric study on vehicle fuel economy and optimization criteria of the pleated air filter designs to improve the performance of an I.C diesel engine: Experimental and CFD approaches. *Separation and Purification Technology*.

Caesar, T. and Schroth, T., 2002. The influence of pleat geometry on the pressure drop in deep-pleated cassette filters. *Filtration and Separation*.

Cambridge Filter Corporation, 2006. *Absolute Filter THINFIL (Low Profile) Mini-Pleat HEPA Filter Product Sheet*.

Cengel, Y. and Cimbala, J., 2012. *Fluid Mechanics Fundamental and Aplication Third Edition*. *Foreign Affairs*.

Chen, D.R., Pui, D.Y.H. and Liu, B.Y.H., 1995. Optimization of pleated filter designs using a finite-element numerical model. *Aerosol Science and Technology*.

Debaun, K.W., 1966. *Pleated Air Filter Catridge*.

Durksen, S., 2019. *SOLIDWORKS 2020 Hardware FAQs and Recommendations*. [online] Solidworks Tech Tip. Available at: <https://www.javelin-tech.com/blog/2019/10/solidworks-2020-hardware-recommendations/> [Accessed 12 Sep. 2020].

Dynamic Air Quality Solutions, 2020. *The Importance of IAQ - Dynamic Air Quality Solutions / Residential*. [online] Available at: <https://www.dynamicaqs.com/residential/index.php?option=com_content&view=article&id=57&Itemid=495> [Accessed 21 Apr. 2020].

EMW, 2020. *Effective Filter Media Area*. [online] Available at: <https://www.emw.de/en/filter-campus/effective-filter-media-area.html> [Accessed 21 Apr. 2020].

EngineerEdge, 2020. *HEPA Air Filter Construction - Engineers Edge*. [online] Available at: <https://www.engineersedge.com/filtration/hepa_filter_construction.htm> [Accessed 21 Apr. 2020].

Fu, H.M., Fu, Y. and Xu, F., 2014. Experiment and simulation on pressure drop of pleated air filters. *Advanced Materials Research*, 960–961(July), pp.568–573.

Kelley, M., 2019. *The Importance of Counting 2.5um Particles in Hospital Operating Rooms*. [online] Available at: <https://www.setra.com/blog/the-importance-of-counting-2.5um-particles-in-hospital-operating-rooms> [Accessed 21 Apr. 2020].

Lydall, 2016. *Arioso M7001-G1 Typical Property Sheet*.

Maddineni, A.K., Das, D. and Damodaran, R.M., 2019. Numerical investigation of pressure and flow characteristics of pleated air filter system for automotive engine intake application. *Separation and Purification Technology*.

Oransi, 2020. *HEPA Filter - The Complete Guide Oransi*. [online] Available at: <https://www.oransi.com/page/what-is-a-hepa-filter> [Accessed 21 Apr. 2020].

Oughton, D., 2014. *Faber & Kell's Heating and Air-Conditioning of Buildings*. *Faber & Kell's Heating and Air-Conditioning of Buildings*.

Ozen Engineering Incorporation, 2020. *ANSYS System Hardware Requirements*. [online] Available at: <https://www.ozeninc.com/ansys-system-hardware-requirements/> [Accessed 12 Sep. 2020].

Patil, S.R. and Lomte, P.S. V, 2015. Design and development of high performance panel air filter with experimental evaluation and analysis of filter media pleats. *Int. Journal of Engineering Research and Applications*, 5(11), pp.47–51.

Permatron, 2020. *Air Filter Media*. [online] Available at: <https://www.permatron.com/air-filter-media> [Accessed 21 Apr. 2020].

Schousboe, F.C., 2017. Media Velocity Considerations in Pleated Air Filtration. *Graduate Theses and Dissertations*. [online] Available at: <http://scholarcommons.usf.edu/etdhttp://scholarcommons.usf.edu/etd/6632>.

Sipes, J., 2011. *BASICS OF AIR FILTRATION*.

Tronville, P. and Sala, R., 2003. Minimization of resistance in pleated-media air filter designs: Empirical and cfd approaches. *HVAC and R Research*.

Wiegmann, A., Cheng, L., Glatt, E., Iliev, O. and Rief, S., 2009. Design of pleated filters by computer simulations. 155(155).

Zhang, A., 2018. *The introduction of air filter – Filmedia Home*. [online] Available at: <http://www.best-filter.com/the-introduction-of-air-filter/#respond> [Accessed 21 Apr. 2020].

APPENDICES

APPENDIX A: Absolute Filter THINFIL Minipleat Product Sheet

Figure A-1: Overview of Absolute Filter THINFIL Minipleat

Standard Specifications
Applicable to both Standard and "Silver Seal" Filters

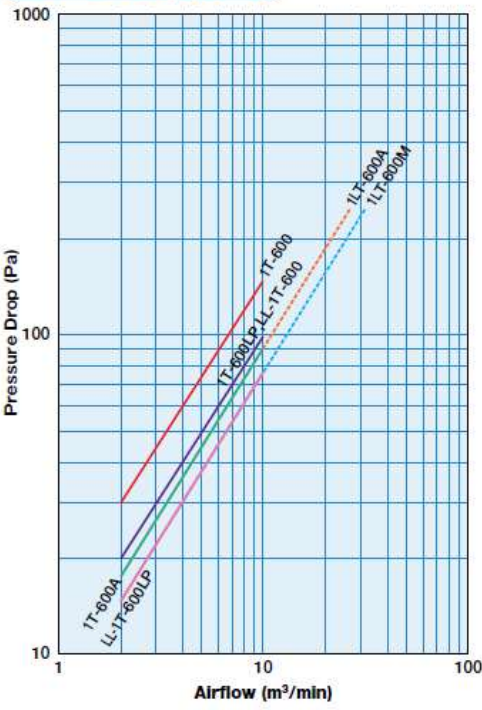| Model	Rated Airflow Volume (m³/min)	Pressure Drop (Pa) Initial Max.	Final	External Dimensions (mm) Height	Width	Depth	Weight (kg)
1T-50E	0.44			203	203		0.5
1T-110E	1.1	83		305	305	35	0.8
1T-320E	2.3			610	305		1.3
1T-600E	5.0			610	610		2.1
1T-320	4.7			610	305		1.5
1T-600	10.0	147		610	610	50	2.5
1T-830	12.7			610	762		3.0
1T-960	15.3			610	915		3.5
1T-320LP	4.7			610	305		2.0
1T-600LP	10.0	98	294	610	610	65	3.3
1T-830LP	12.7			610	762		4.0
1T-980LP	15.3			610	915		4.7
1T-320A	4.7			610	305		2.3
1T-600A	10.0	88		610	610	80	3.9
1T-830A	12.7			610	762		4.7
1T-980A	15.3			610	915		5.5
1T-320M	4.7			610	305		3.0
1T-600M	10.0	74		610	610	100	5.1
1T-830M	12.7			610	762		6.2
1T-980M	15.3			610	915		7.3

Custom sizes available. Please contact us for more information.

High Airflow Volume
LL-Type available in 99.97% efficiency only. Standard and "Silver Seal" 1LT Filters available.

Model	Rated Airflow Volume (m³/min)	Pressure Drop (Pa) Initial Max.	Final	External Dimensions (mm) Height	Width	Depth	Weight (kg)
LL-1T-320	4.7			610	305		1.7
LL-1T-600	10.0	98		610	610	50	2.8
LL-1T-830	12.7			610	762		3.4
LL-1T-960	15.3		294	610	915		4.0
LL-1T-320LP	4.7			610	305		2.1
LL-1T-600LP	10.0	78		610	610	65	3.6
LL-1T-830LP	12.7			610	762		4.3
LL-1T-980LP	15.3			610	915		5.1
1LT-320A	12.8			610	305		2.3
1LT-600A	27.0	249		610	610	80	3.9
1LT-830A	34.1			610	762		4.7
1LT-980A	41.2		498	610	915		5.5
1LT-320M	15.1			610	305		3.0
1LT-600M	32.0	249		610	610	100	5.1
1LT-830M	40.0			610	762		6.2
1LT-980M	48.8			610	915		7.3

Custom sizes available. Please contact us for more information.

Component Materials / Usage Specifications

Models		All
Component Materials	Media	Glass Fiber
	Separator	Hot Melt Resin
	Frame	Aluminum
	Frame Finish	Anodized Aluminum + Clear Acrylic Coating
	Sealant	Urethane Resin
	Gasket	Chloroprene
Usage Specifications	Max. Continuous Operation Temperature (C)	60
	Max. Peak Humidity (%RH at 0 Condensation)	100

11

Figure A-2: Specifications of Absolute Filter THINFIL Minipleat

APPENDIX B: Lydall Arioso M7001-G1 Typical Property Sheet

M7001-G1
TYPICAL PROPERTY SHEET

◇Lydall

Arioso®
HIGH PERFORMANCE AIR FILTRATION
COMPOSITE MEDIA

Partners in Performance

For Gas Turbine and Critical Air Filtration Applications

Combining high filtration efficiencies with an extremely low pressure drop, *Arioso*® M70 Series High Performance Air Filtration Composite Media is designed to lower operating and maintenance costs on gas turbines, while ensuring high power output. Its low resistance and mechanical filtration makes it ideal for critical air filtration applications.

The proprietary technology for *Arioso* media incorporates a *Solupor*® membrane made from UPE (ultra-high molecular weight polyethylene), a chemically inert and highly durable polymer. This membrane is laminated to a support layer to form a composite that is mechanically robust.
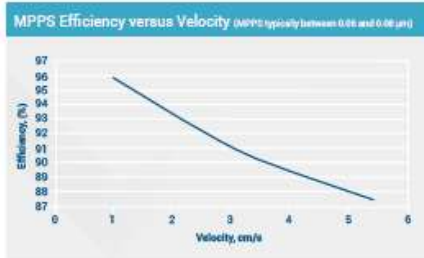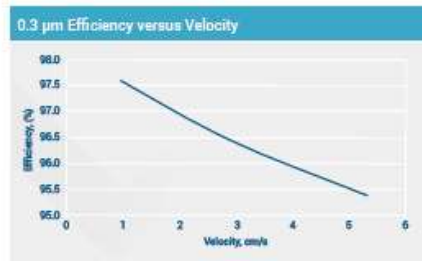
Typical Air Filtration Properties (TSI Model 3160 CNC)

Typical Properties	US Customary Units		SI Units		Reference Test Methods
Filter Class	MERV 15/16	ASHRAE 52.2	F9	EN779	Flat Sheet
Efficiency (0.3µm DEHS @ 5.33 cm/s)	95.4	%	95.4	%	MIL-STD-282 A.S.T.M. - D2986-91
Penetration (0.3µm DEHS @ 5.33 cm/s)	4.6	%	4.6	%	MIL-STD-282 A.S.T.M. - D2986-91
MPPS Efficiency (0.3µm DEHS @ 5.33 cm/s)	87.5	%	87.5	%	MIL-STD-282 A.S.T.M. - D2986-91
MPPS Penetration (0.3µm DEHS @ 5.33 cm/s)	12.5	%	12.5	%	MIL-STD-282 A.S.T.M. - D2986-91
Air Resistance (5.33 cm/s)	4.6	mm H_2O	45	Pa	MIL-STD-282 A.S.T.M. - D2986-91
Air Permeability/Frazier (125 Pa)	33	ft³/ft²/min	16.8	cm³/cm²/s	TAPPI T - 251

Lydall Performance Materials   www.lydallpm.com

Figure B-1: Typical Air Filtration Properties (TSI Model 3160 CNC)

M7001-G1 Typical Property Sheet

Typical Physical Properties of Arioso® Composite

Typical Properties	US Customary Units		SI Units		Reference Test Methods
Functional Support Layer	Glass, Wet-Laid		Glass, Wet-Laid		
Basis Weight	34.1	lbs/3000 ft²	55	g/m²	T.A.P.P.I. - T - 410 A.S.T.M. - D -646
Gurley Stiffness (MD)	650	mgf	650	mgf	T.A.P.P.I. - T - 543
Thickness/Caliper (7.3psi / 50 kPa)	13.6	mils	0.34	mm	T.A.P.P.I. - T - 411
Water Repellency	28	in. wg	711	mm wg	MIL STD 282
Continuous Operating Temperature	176	°F	80	°C	Max

Resistance versus Velocity

0.3 μm Efficiency versus Velocity

MPPS Efficiency versus Velocity (MPPS typically between 0.08 and 0.08 μm)

Note: All product data is nominal and does not represent a specification.

All data and statements concerning these products may be considered as being indicative of representative properties and characteristics obtainable. We make no warranty, expressed or implied, concerning actual use or results because of industry specific influences.

◇ **Lydall**
Partners
In Performance

Lydall Performance Materials   www.lydallpm.com

info@lydall.com   North America & Asia: +1 603 332 4600   Europe, Middle East & Africa: +33 (0) 2 97 28 5300

Rev. Date: 02/03/2016   All rights reserved. Copyright 2016

Figure B-2: Typical Physical Properties of Arioso Composite